ENHANCING PERFORMANCE OF PAPER COATINGS BY TAILOR-MADE PLASTIC PIGMENTS

Mia Ahokas

Åbo Akademi University

Laboratory of Polymer Technology
Center for Functional Materials (FunMat)
Department of Chemical Engineering
Division for Natural Sciences and Technology
Åbo Akademi University
Turku/Åbo, Finland 2011

PRINTED INTELLIGENCE
FUN MAT
FUNCTIONAL MATERIALS

Enhancing performance of paper coatings by tailor-made plastic pigments

Mia Ahokas

Academic Dissertation

Laboratory of Polymer Technology
Center for Functional Materials (FunMat)
Department of Chemical Engineering
Division for Natural Sciences and Technology
Åbo Akademi University
Turku/Åbo, Finland 2011

Supervisor and Custos
Prof. Carl-Eric Wilén
Laboratory of Polymer Chemistry
Department of Chemical Engineering
Åbo Akademi University
Åbo, Finland

Opponent and Reviewer
Prof. Patrick Gane
Printing Technology
Department of Forest Products Technology
Aalto University
Helsinki, Finland

Reviewer
Prof. Jurkka Kuusipalo
Institute of Paper Converting
Department of Energy and Process Engineering
Tampere University of Technology
Tampere, Finland

ISBN 978-952-12-2599-4 (print)
ISBN 978-952-12-2600-7 (electronic)

Painosalama Oy
Turku, Finland 2011

“Blessed are the curious
for they shall have adventures.”
-Lovelle Drachman

Preface and acknowledgments

This thesis is based on research work carried out at the Laboratory of Polymer Technology, Åbo Akademi University. I also had the opportunity of working one summer at Topchim, Wommelgem, Belgium. For financial support the Finnish Funding Agency for Technology and Innovation (TEKES), the Center for Functional Materials (FunMat), the Research Institute of Åbo Akademi Foundation, the Rector of Åbo Akademi, Topchim and former Ciba Speciality Chemicals are all gratefully acknowledged.

I am thankful to my supervisor Professor Carl-Eric Wilén for giving me the opportunity to work with this exciting subject and for his support and creative ideas throughout my work. I would also like to thank Assistant Professor Ari Rosling for his guidance, Dr. Hendrik Luttikhedde for fruitful discussions and Mr. Henk Van den Abbeele for collaboration and kind hospitality I received in Belgium. I am also honored to have Professor Patrick Gane as my opponent and reviewer and Professor Jurkka Kuusipalo as my reviewer.

Additionally, I would like to thank all my colleagues and staff at the Laboratory of Polymer Technology for a nice working environment. Special thanks to Mr. Johan Norrgård for assistance and Mr. Roger Nordqvist and Mr. Carl-Johan Wikman for equipmenting and Mrs. Päivi Pennanen for guidance with NMR. Also special recognitions are owed to Mrs. Maria Pinjanainen and Ms. Marian Lundenius for their efforts. Furthermore, I would like to thank the personnel at former Ciba Speciality Chemicals and Topchim for the collaboration and support.

I am always grateful to my friends for entertaining me in my leisure time and giving me good counterbalance to work. Thank you for not forgetting me!

Finally, I want to express my deepest gratitude to my family. Especially, thanks to my Mom and Dad for your endless support and encouragement throughout my long journey to this point. Janne, thank you for being there for me and loving me through ups and downs of life.

Turku, May 2011

Mia Ahokas

Abstract

Enhancing performance of paper coatings by tailor-made plastic pigments

by Mia Ahokas

Keywords: *paper coating, plastic pigments, core-shell polymers, polyimides, organic-inorganic hybrids*

The paper industry is constantly looking for new ideas for improving paper products while competition and raw material prices are increasing. Many paper products are pigment coated. Coating layer is the top layer of paper, thus by modifying coating pigment also the paper itself can be altered and value added to the final product.

In this thesis, synthesis of new plastic and hybrid pigments and their performance in paper and paperboard coating is reported. Two types of plastic pigments were studied: core-shell latexes and solid beads of maleimide copolymers. Core-shell latexes with partially crosslinked hydrophilic polymer core of poly(*n*-butyl acrylate-*co*-methacrylic acid) and a hard hydrophobic polystyrene shell were prepared to improve the optical properties of coated paper. In addition, the effect of different crosslinkers was analyzed and the best overall performance was achieved by the use of ethylene glycol dimethacrylate (EGDMA). Furthermore, the possibility to modify core-shell latex was investigated by introducing a new polymerizable optical brightening agent, 1-[(4-vinylphenoxy)methyl]-4-(2-phenylethylenyl)benzene which gave promising results. The prepared core-shell latex pigments performed smoothly also in pilot coating and printing trials. The results demonstrated that by optimizing polymer composition, the optical and surface properties of coated paper can be significantly enhanced.

The optimal reaction conditions were established for thermal imidization of poly(styrene-*co*-maleimide) (SMI) and poly(octadecene-*co*-maleimide) (OMI) from respective maleic anhydride copolymer precursors and ammonia in a solvent free process. The obtained aqueous dispersions of nanoparticle copolymers exhibited glass transition temperatures (T_g) between 140-170ºC and particle sizes from 50-230 nm. Furthermore, the maleimide copolymers were evaluated in paperboard coating as additional pigments. The maleimide copolymer nanoparticles were partly imbedded into the porous coating structure and therefore the full potential of optical property enhancement for paperboard was not achieved by this method.

The possibility to modify maleimide copolymers was also studied. Modifications were carried out via *N*-substitution by replacing part of the ammonia in the imidization reaction with amines, such as triacetonediamine (TAD), aspartic acid (ASP) and fluorinated amines (2,2,2-trifluoroethylamine, TFEA and 2,2,3,3,4,4,4-heptafluoro-buthylamine, HFBA). The obtained functional nanoparticles varied in size between 50-217 nm and their T_g from 150-180ºC. During the coating process the produced plastic pigments exhibited good runnability. No significant improvements were achieved in light stability with TAD modified copolymers whereas nanoparticles modified with aspartic acid and those containing fluorinated groups showed the desired changes in surface properties of the coated paperboard.

Finally, reports on preliminary studies with organic-inorganic hybrids are presented. The hybrids prepared by an *in situ* polymerization reaction consisted of 30 wt% poly(styrene-*co*-maleimide) (SMI) and high levels of 70 wt% inorganic components of kaolin and/or alumina trihydrate. Scanning Electron Microscopy (SEM) images and characterization by Fourier Transform Infrared Spcetroscopy (FTIR) and X-Ray Diffraction (XRD) revealed that the hybrids had conventional composite structure and inorganic components were covered with precipitated SMI nanoparticles attached to the surface via hydrogen bonding. In paper coating, the hybrids had a beneficial effect on increasing gloss levels.

Sammanfattning

Mervärde för pappersbestrykning genom skräddarsydda plastpigment

av Mia Ahokas

Nyckelord: *pappersbestrykning, plastpigment, core-shell polymer, polyimider, organisk-oorganiska hybrider*

Pappersindustrin letar efter nya idéer för att ge mervärde för papper emedan konkurrens och priser på utgångsmaterial ökar. En stor del av pappersprodukter är bestrykta. Bestrykningsskiktet är det yttersta skiktet hos pappret således genom att modifiera bestrykningspigmenten kan vi också modifiera papper och ge mervärde för den slutliga produkten.

I denna avhandling rapporterades synteser av nya plastpigment och hybrider samt deras beteende i pappers- och kartongsbestrykningen. Två typer av plastpigment undersöktes: core-shell latex och maleimid sampolymerer. Core-shell latex med en partiell tvärbunden hydrofil polymer kärna av poly(*n*-butylakrylat-*co*-metakrylsyra) och ett hårt hydrofobt polystyren skal preparerades för att förbättra optiska egenskaper hos bestruket papper. Även inverkan av olika tvärbindare undersöktes och det bästa resultatet uppnåddes med etylen glykol dimetakrylat (EGDMA). Därtill utreddes möjligheten att modifiera core-shell latex mha nytt polymeriserbart optiskt vitmedel 1-[(4-vinylfenoxy)metyl]-4-(2-fenyletylenyl)bentsen med lovande resultat. De tillverkade core-shell latex pigmenten klarade sig bra även i pilot bestrykning och tryckning. Resultat demonstrerade att genom optimering av polymersammansättningen kunde man markant öka de optiska egenskaperna samt ytslätheten hos bestruket papper.

De optimala reaktionsbetingelserna karakteriserades för termisk imidisering av poly(styren-*co*-maleimid) (SMI) och poly(octadecen-*co*-maleimid) (OMI) från respektive maleic anhydrid sampolymerer med ammoniak i en lösningsmedelsfri reaktion. De erhållna vattenbaserade dispersionerna av sampolymer nanopartiklar visade glassomvandlingstemperaturer (T_g) mellan 140-170ºC och partikelstorlek mellan 50-230 nm. Maleimid sampolymerer evaluerades också i bestrykningen av kartong som tilläggspigment. Nanopartiklarna blev delvis inbäddade i den porösa bestrykningsstrukturen och därmed kunde inte nyttan i de optiska egenskaperna uppnås fullständigt i kartong med dessa maleimid sampolymer nanopartiklarna.

Vi undersökte möjligheten att modifiera även maleimid sampolymerer. Modifieringarna fullgjordes genom *N*-substituering med delvis ersättning av ammoniak med primära aminer så som triacetonediamine (TAD), aspartic syra (ASP) och fluorerade aminer (2,2,2-trifluoroetylamin, TFEA och 2,2,3,3,4,4,4-heptafluorobutylamin HFBA) i imidiseringreaktionen. De erhållna funktionella nanopartiklarna varierade i storleken mellan 50-217 nm och deras T_g mellan 150-180ºC. Genom fluorinerade grupper och aspartic syra modifierade nanopartiklar visade förändringar i ytegenskaperna hos bestruken kartong som förväntat emedan inga markanta förbättringar i ljusstabiliteten uppnåddes genom TAD modifierade sampolymerer. Därtill hade plastpigmenten bra körbarhet i bestrykningsprocessen.

Till sist presenterades resultat från preliminära experiment med organisk-oorganiska hybrider med 30 vikts-% poly(styren-*co*-maleimid) och höga halter av 70 vikts-% oorganiska komponenter av kaolin och alumina trihydrat tillverkade genom *in situ* polymerisering. Skanning Elektron Mikroskopi (SEM) bilder av hybrider visade att hybrider med den konventionella kompositstrukturen hade oorganiska komponenter täckta genom väte-bindningar fästade SMI nanopartiklar på ytan vilket karakteriserades med Fourier Transform Infraröd Spektroskopi (FTIR) och Röntgendiffraktion (XRD). I pappersbestrykningen ökade hybrider glansvärdena.

List of original publications

This thesis is based on the following publications:

I. Koskinen, M.; Wilén, C-E. **Preparation of core-shell latexes for paper coatings.** *Journal of Applied Polymer Science* (2009) 112: 1265-1270.

II. Ahokas, M.; Wilén, C-E. **Synthesis of poly(styrene-co-maleimide) and poly(octadecene-co-maleimide) nanoparticles and their utilization in paper coating.** *Progress in Organic Coatings* (2009) 66: 377-381.

III. Ahokas, M.; Wilén, C-E. **Modified and functionalized maleimide copolymers for paper coatings.** *Polymer Bulletin* (2011) 66: 491-501.

IV. Ahokas, M.; Wilén, C-E. **Hybrid coating pigments of poly(styrene-co-maleimide)/kaolin/alumina trihydrate for paper coating.** *Progress in Organic Coatings* (2011). Accepted for publication. DOI: 10.1016/j.progcoat.2011.03.021

Abbreviations

ASP	aspartic acid
ATH	alumina trihydrate
BA	*n*-butyl acrylate
CMC	carboxymethyl cellulose
DLS	dynamic light scattering
DMF	*N,N*-dimethylformamide
DMSO	dimethyl sulfoxide
DSC	differential scanning calorimetry
DST	dynamic surface tension
EB	ethylbenzene
EGDMA	ethylene glycol dimethacrylate
FTIR	Fourier transform infrared spectroscopy
FWA	fluorescent whitening agent
GCC	ground calcium carbonate
HALS	hindered amine light stabilizer
HFBA	heptafluorobuthylamine
HWC	high weight coated paper
K	kaolin
LWC	light weight coated paper
MAA	methacrylic acid
MBA	*N,N*-methylene bisacrylamide
MEK	methyl ethyl ketone
MI	maleimide
MMT	montmorillonite
MWC	medium weight coated paper
NMF	*N*-methylformamide
NMR	nuclear magnetic resonance spectroscopy
OBA	optical brightening agent
OMA	poly(octadecene-co-maleic anhydride)
OMI	poly(octadecene-co-maleimide)
PCC	precipitated calcium carbonate
PCN	polymer-clay nanocomposites
PPS	Parker Print Surf method
RFID	radio frequency identification
RH	relative humidity
S	styrene
SEC	size-exclusion chromatography
SEM	scanning electron microscopy
SMA	poly(styrene-co-maleic anhydride)
SMI	poly(styrene-co-maleimide)
T_g	glass transition temperature
TAD	triacetonediamine
TEM	transmission electron microscopy
TFEA	trifluoroethylamine
THF	tetrahydrofuran
TMPTA	1,1,1-trimethylol propane triacrylate
XRD	X-ray diffraction
ÅA-GWR	Åbo Akademi gravimetric water retention

Table of contents

Preface and acknowledgments ..... **i**

Abstract ..... **ii**

Sammanfattning ..... **iv**

List of original publications ..... **vi**

Abbreviations ..... **vii**

Table of contents ..... **viii**

1. Introduction **1**

2. Background **2**

2.1 Paper coating pigments **3**

2.1.1 Inorganic coating pigments **4**

2.1.2 Organic coating pigments **8**

2.1.3 Organic-inorganic hybrids **20**

2.2 Aim of the study **27**

3. Experiments **28**

3.1 Synthesis **28**

3.1.1 Synthesis of core-shell latexes **28**

3.1.2 Synthesis of maleimide copolymer pigments **29**

3.1.3 Synthesis of organic-inorganic hybrids **30**

3.2 Methods **31**

3.2.1 Coating color preparation **31**

3.2.2 Coating applications **32**

3.2.3 Polymer analysis **33**

3.2.4 Coating color and paper analysis **35**

4. Results and discussions **36**

4.1 Polymer characterization **36**

4.1.1 Core-shell latexes (Paper I) **36**

4.1.2 Maleimide copolymers (Papers II-III) 37
4.1.3 Organic-inorganic hybrids (Paper IV) 41
4.2 Effect of synthetic pigments on paper coating 44
4.2.1 Effect of core-shell pigments (Paper I) 44
4.2.2 Effect of maleimide copolymers (Paper II) 48
4.2.3 Effect of modified maleimide copolymers (Paper III) 49
4.2.4 Effect of organic-inorganic hybrids (Paper IV) 52
5. Conclusions 54
6. References 56
Original papers 61

1. Introduction

Paper is an important medium for communication, education, artistic products, packaging, sanitary and technical applications. Paper products make our daily lives easier. Paper and paperboard have a strong position in the market. According to a report by the Finnish Forest Industries Federation, the annual global production volume is 370 million tonnes of which Finland produced 11.8 million tonnes in 2010. The average global consumption of paper per capita is 55 kg, whereas in Finland the figure is 230 kg per capita, thus there is still growth potential in the global market. Nonetheless, the paper industry finds itself facing new challenges with fierce competition and increasing raw material and energy costs. In addition, the concern for environmental issues is growing.

One challenge for the paper industry today is to find its own role in the electronic sector. Integrating new materials into paper products creates significant opportunities for the paper producer. Smart papers already exist with incorporated electronic capability achieved through conductive inks or polymers on top of paper or board resulting in products such as smart labels, tickets, radio frequency identification (RFID) tags and sensors. Innovation holds the key to survival. Novel ideas are needed to introduce new products to the market with added value that combine better properties with cost effectiveness.

Many paper products are coated in order to improve paper quality. Coated papers are produced both from mechanical and chemical pulp and prepared in light weight coated (LWC), medium weight coated (MWC) and high weight coated (HWC) grades. Coated paper and paperboard products are used in printing, writing, catalogues, magazines, art papers and packaging applications.

The coating layer is the top most layer of the paper and thus affects the surface properties of the paper. Most of the coating comprises of pigments and therefore by tailor-making pigments, the surface properties of the paper can be fine-tuned. By modifying pigments with functional groups, new functionality and value can potentially be added to the paper product. In this thesis, we have studied and modified different plastic pigments in order to improve paper properties. Furthermore, the utilization of a hybrid technique in paper coating was examined for exploiting synergy of organic and inorganic components.

2. Background

In the coating of paper, an aqueous suspension of coating color is applied on paper. After application the coating is dried and finished, usually by calendering to give paper the final smoothness and gloss. The main objective of paper coating is to improve paper quality. Scanning electron microscope (SEM) images of coated and uncoated paper surfaces are shown in Figure 1. The appearance is clearly different for coated and uncoated papers. Optical properties and quality of the coated paper are improved by filled cavities, covered fibers and smoothened paper surface. Also, one of the most important functions of paper coating is providing better printing in terms of print quality, image reproduction, printability and surface strength. Coating generally decreases stiffness and ink absorption and increases properties such as gloss, opacity and both surface and mechanical strength of the paper. Although a great deal can be achieved by paper coating, naturally, many properties of the final product depend strongly on the base paper itself.[1-3]

Coating color consists of mainly pigments, binders, thickeners and various additives. The most important component in the coating color is pigment which in a dry coating layer makes up to 80-95 wt% of the total coating weight. Pigments are either inorganic minerals or synthetic organic pigments. Binders, by definition, bind pigments to base paper and each other. One or more binders are added in 5-20 wt% to the coating color. Polymer based dispersions are commonly used as binders and their contribution is crucial in creating surface strength for paper coating. Thickeners, also synthetic or natural polymers, on the other hand, are added to modify the rheology and water retention of the coating color. Rheological properties of the coating color greatly affect runnability and thus production efficiency.[1,4,5]

In addition to solid materials, the dried coating layer also contains pores, air-filled spaces and capillaries. These play a central role for ink absorption. Porosity is adjusted by choosing a set of different particle shapes and sizes. The relationship between particle diameter and thickness is defined as the aspect ratio and it expresses the degree of platiness of the particle. Common paper coating particle shapes are spherical (aspect ratio 1), rod/needle-like (aspect ratio 5-20) or platy (aspect ratio 20-200) depending on the pigment type. In addition, the percentage by weight of particles with a particle size less than 2 μm rather than the average particle size is often reported. Besides particle size, shape and distribution, other pigment properties, *e.g.* density, refractive index, light

scattering and light absorption also affect paper properties such as gloss, opacity, brightness, ink absorption, porosity and bulk. Thus, when choosing a certain type of pigment one actually selects a set of properties for the coating.[1,6-8]

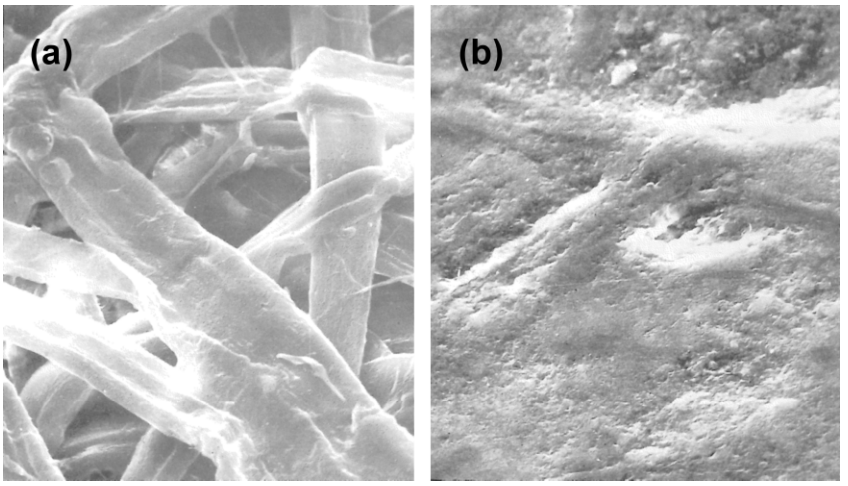

Figure 1: Scanning electron microscope images of (a) uncoated and (b) coated paper surfaces.[1]

2.1 Paper coating pigments

Paper coating pigments can be divided into three groups based on their usage: (1) main pigments, (2) special pigments and (3) additional pigments. The main pigments form the major fraction of a coating color, but special pigments may also be used, though their utilization is limited to special applications. Additional pigments are inserted to supplement properties of the main pigment in fraction usually up to ~10 wt%. The most common main pigments are kaolin (K), ground calcium carbonate (GCC) and talc, gypsum is an example of special pigment and precipitated calcium carbonate (PCC), titanium dioxide (TiO_2), alumina trihydrate (ATH) and plastic pigments are all well-known additional pigments. Pigments can also be classified according to their origin into inorganic and organic pigments. Organic-inorganic hybrids are still quite rare among paper coating pigments. In this chapter, certain aforementioned pigments will be presented.[1,2]

2.1.1 Inorganic coating pigments

Kaolin

Kaolin is a widely occurring mineral used by paper industry both as filler and coating pigment.[6,9] Kaolin is uniquely suited for this use because of its fine particle size, platy pseudo-hexagonal particle shape, good viscosity, low abrasion, good opacity, white color, high brightness and good printability.[2,10] Kaolin clay consists mainly of the mineral kaolinite. (The chemical composition of kaolinite will be discussed in detail in section 2.1.3.) Kaolin deposits are classified either as primary or secondary. Primary kaolins are formed from residual weathering or hydrothermal alteration whereas secondary kaolins are sedimentary in origin. The largest deposits that are utilized by the paper industry are located in Georgia, USA (secondary), Cornwall, UK (primary) and the lower Amazon basin in Brazil (secondary). Some specific characteristics are dependent on the geographical source.[1,10] One major distinction between US and UK clay is the difference in aspect ratio which in general for US clay is 5-15 and for UK clay 35-40, thus English kaolins also have a relatively high viscosity in comparison with sedimentary kaolins.[10,11]

Kaolin particles agglomerate in stacks of tactoids which can be seen in Figure 2. In aqueous medium the faces of the kaolin particles are always negatively charged while the edges have positive charge at acidic conditions and negative charge at alkaline conditions. When kaolin powder is mixed with water and an anionic dispersing agent, the dispersing agent is adsorbed by the edges preventing agglomeration by electrostatic and steric hindrance and resulting in a stable dispersion.[1] Nowadays there are several processes that can be utilized for fine-tuning different kaolin grades. These products are generally designated as engineering clays. The processes that can be used to alter kaolin products are centrifugation, delamination, magnetic separation, flotation, selective flocculation, chemical leaching, pulverization, blending, calcination and chemical structuring.[9] Delamination is a process in which stacks of kaolin are separated by shearing into individual platelets, *i.e.* thinner platelet particles of equal or finer diameter than the original stack. In flotation, substantial portions of titanium, quartz and other bearing mineral contaminants are removed from kaolin resulting in high brightness products. In the calcination process kaolin is first heated to 500-700°C at which kaolinite mineral dehydroxylates and the crystal structure breaks down to metakaolin. Upon further heating to 900-1000°C, metakaolin reorganizes to form small crystals that aggregate to form

particles with an open structure that have relatively high light scattering coefficient. These calcined kaolin products have a high brightness of 92-94% whereas regular kaolin particles have a brightness from 84-88% and particle sizes range from 70-90 wt% < 2 µm. Key properties which can be positively enhanced by coating with kaolins include gloss, brightness, opacity, smoothness and print properties. The product is generally delivered to the paper mill as powder or slurry at 65% solids content or higher.[1,9,11]

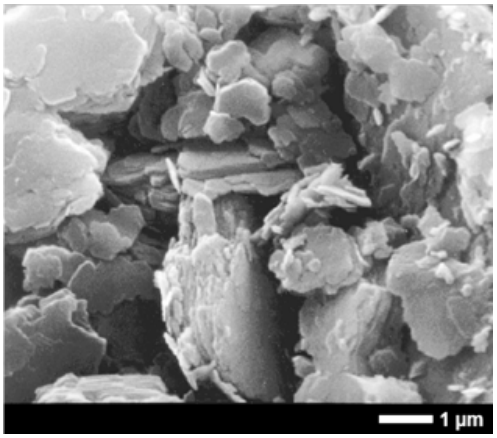

Figure 2: Scanning electron microscope image of kaolin.[11]

Calcium carbonate

The major competitive mineral for kaolin in the paper industry is calcium carbonate ($CaCO_3$) with good price to performance ratio. Natural $CaCO_3$ deposits occurring globally are based on rocks of chalk, limestone or marble.[2] There are two routes for preparing calcium carbonate: specific grinding of $CaCO_3$ producing ground calcium carbonate (GCC) or chemical precipitation of $CaCO_3$ resulting in precipitated calcium carbonate (PCC).[1,11-13] GCC is mainly ground from limestone or marble deposits whereas PCC is predominantly prepared from limestone.[12] In the precipitation process, the first step is calcination of limestone to lime (CaO) and carbon dioxide gas (CO_2). Lime is then further hydrated with water to calcium hydroxide ($Ca(OH)_2$) and the last phase constitutes of re-carbonation of $Ca(OH)_2$ with CO_2 resulting in chemically precipitated $CaCO_3$.[1,12,14]

Although the chemical composition of PCC and GCC is the same, nonetheless, differences between these two calcium carbonate grades exist. PCC tends to be a more pure grade for there are several steps in the precipitation process where calcium carbonate can be purified thereby removing much of the impurities from the deposit that cannot be

separated in grinding. In addition, PCC processing allows preparing crystals in different shapes such as clustered needles, cubes, prisms and scalenohedrons besides rhombohedrons which is the dominant form of GCC. PCC particle shape is dictated by the process parameters affecting both structure and physical properties. Thus, PCC is a versatile pigment and is used as additional pigment whereas GCC is added as main pigment in the coating color.[1,12]

Application of calcium carbonates requires neutral or alkaline pH since $CaCO_3$ dissolves under acidic conditions.[1,14] The reasons for increased interest for calcium carbonates include improved brightness, good rheological properties and cost-savings.[1,12] Typically, GCC and PCC have high ISO-brightness of above 90%. GCC particle size ranges from 40-98 wt% < 2 μm and shows excellent rheological behavior.[1] PCC has narrower particle size distribution than GCC as can be seen in Figure 3 and also greater variety in different shapes and sizes available. The solids content of the calcium carbonate slurry which is the main form of delivery can be up to ≥ 78 wt%.[12] Production sites are within relatively close distances to the paper mills due to wide occurrence of the deposits and calcium carbonates can be supplied over an efficient logistic chain.[1]

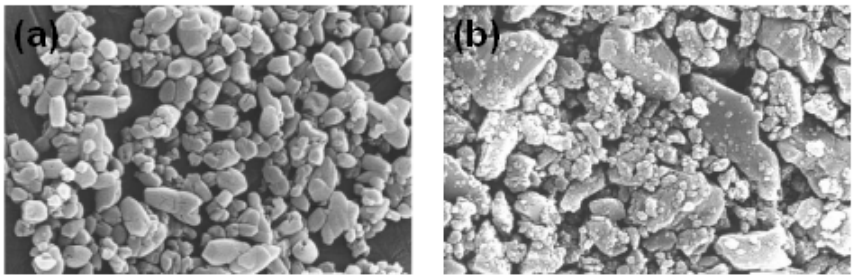

Figure 3: Scanning electron microscope images of (a) precipitated calcium carbonate (PCC) and (b) ground calcium carbonate (GCC).[12]

Alumina trihydrate

Alumina trihydrate (ATH), also known as hydrated alumina, is a crystalline aluminum hydroxide $Al(OH)_3$ with a crystal lattice structure of mineral gibbsite.[15] It is produced by the Bayer process from bauxite ore, for paper industry mainly in Australia and Guinea in Africa.[1] In the Bayer process, impurities such as iron oxides and silicates are removed and during the precipitation step particle size can be controlled.[1,2,15]

The bonds between aluminum and hydroxyl ions in ATH are predominantly ionic and the hydroxyl groups are essentially equivalent. Upon heating to temperatures above 220ºC, ATH decomposes endothermically to alumina by releasing 35 wt% water. This ability to absorb heat and release water vapor is the principal action mechanism for ATH as flame retardant which constitutes its major market.[1,15]

ATH is supplied as powder or as slurry at 65-70% solids content to the paper mills. ATH grades used in paper coating have platy pseudo-hexagonal particles of roughly 1µm in diameter with narrow particle size distribution. They are nontoxic, nonhygroscopic and chemically stable with high whiteness and brightness > 95%. In coated paper, ATH is used as an additional pigment to improve whiteness, brightness, opacity, smoothness, gloss and printability. It can be used also as an extender for the more expensive TiO_2.[1,2]

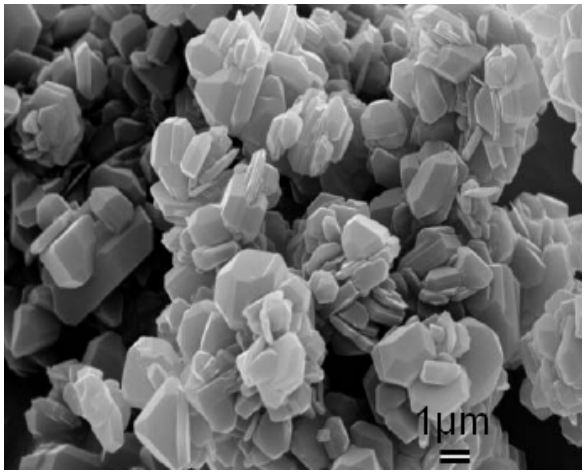

Figure 4: Scanning electron microscope image of aluminta trihydrate, ATH.[16]

2.1.2 Organic coating pigments

Synthetic organic pigments, so-called plastic pigments, are used as additional pigments, generally from 3-20% by dry weight of the main pigment in paper coating, to improve the optical and printing properties of paper and paperboard. Plastic pigments are typically polymeric latexes that differ from binder latexes by having higher glass transition temperatures (T_g), and thus being non-filmforming in the coating process and therefore remaining as discrete particles.[1,2]

Latex polymers are prepared in water by the emulsion technique through free-radical polymerization. Generally plastic pigments can be prepared from a variety of monomers and polymers with glass transition temperature greater than 50ºC.[1] The most popular building block for plastic pigments is based on polystyrene with T_g approximately 100 ºC.[1]

Plastic pigments enhance optical properties of the coating by increasing sheet gloss, brightness and opacity.[1,2,17] Print performance is often improved as a result of increased sheet gloss, smoothness and balance of ink receptivity and ink hold out. One of the important advantages of using plastic pigments is the diminished need for finishing, *i.e.* lower calendering pressure to achieve desired gloss levels. The plastic pigment particles are somewhat thermoplastic and unlike inorganic pigments, they deform slightly upon calendering leading to smoother, less porous and higher gloss surface.[17] Less intense calendering in turn leads to less reduction in paper strength, less compaction of the sheet and thus increased bulk. Also, production efficiency improves through higher calendering speeds. The density of the plastic pigments varies from 0.5 to 1.05 being far below the values of the inorganic pigments that are approximately 2.5. Besides improvements in bulk, this means increased volume solids compared to an equal weight of inorganic pigment.[1]

Plastic pigments are used in coatings whenever improvements in finishing, optical properties or printability are required. General paper grades where plastic pigments can be found include lightweight coated, premium and intermediate grades and coated paperboard. Plastic pigments are delivered to paper mills as dispersion with solids content from 25 to 55%. Particles are uniformly spherical (Figure 5) with a size ranging from 100 nm-1 μm, a refractive index > 1.5 and an extremely high brightness > 98% due to low absorption of electromagnetic radiation in the wide range of 300-1500 nm. There are two general classes of plastic pigments: solid beads and hollow spheres.[17] Solid beads are full

polymeric particles whereas hollow sphere particles contain an air void within their volume.[1] These two types of plastic pigments will be presented in detail below.

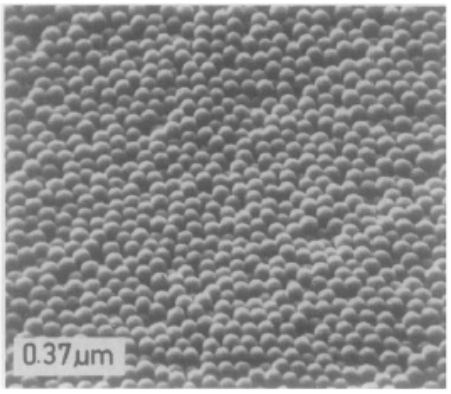

Figure 5: Scanning electron microscope image of polystyrene plastic pigments.[18]

Solid beads

Solid bead plastic pigments are most commonly based on polystyrene (PS) or copolymers thereof.[1,2] Plastic pigments were first introduced by Heiser et al in 1972.[19] An aqueous dispersion of spherical polystyrene plastic pigments was used to improve optical properties of the lightweight coated papers. As a lightweight pigment, plastic pigment was an ideal candidate for this purpose. A coating with solely plastic pigments had similar physical properties compared to a coating with kaolin pigments, and in addition, gloss and brightness were remarkably improved.[19] When used in combination with inorganic pigments, plastic pigments tend to migrate to the top of the coating layer due to the low specific gravity of plastic pigments.[17,19]

Proper selection of particle size for a plastic pigment can lead to increased brightness and opacity. Opacity in a coating is produced when light is both scattered and absorbed as it passes through the coating. Light scatters or refracts as it passes from one medium to another as long as the individual materials have different refracting indexes, the greater the difference the greater the refraction. Thus, most of the light is scattered when light passes from pigment or binder to air and back.[1,20] Refractive index of some pigments is listed in Table 1. From an optical point of view, coating layer can also be considered as a solid matrix of pigments and binders containing dispersed microvoids of air as scattering sites.[18,21] The light-scattering efficiency is a function of the porous structure and drops rapidly with decreased void size.[22] It is generally claimed that the

maximum scattering capacity is obtained when the particle size (or void size) is half of the wavelength of the incident light.[23,24] The spherical plastic pigment particles have an effect on particle packing which can alter size and distribution of air voids that can lead to increased opacity.[1,17,25] According to Alince and Lepoutre,[18] optimum particle size for plastic pigment is 0.4-0.5 µm and optimum pore size is 0.2-0.3 µm although this is also dependent on particle packing and type of mineral pigment used in combination with plastic pigment.[17] Additionally, Lindblad *et al.*[24] noticed that plastic pigments can be used in protection against light-induced discoloration of coated paper products due to the fact that plastic pigments scatter light effectively at the UV wavelength between 290-400 nm which can be detrimental for paper causing loss of brightness and mechanical properties.

Table 1: Refractive index for material in paper coating[1]

Material	*Refractive index*
Kaolin	1.57
Calcium carbonate (PCC)	1.66
Titanium dioxide (TiO_2)	2.76
Alumina trihydrate (ATH)	1.58
Plastic pigment, solid bead (PS)	1.59
Plastic pigment, hollow sphere (PS)	1.0-1.59
Air	1.0

Maleimide copolymers

Maleimide (MI) copolymers, such as poly(styrene-*co*-maleimide) (SMI) or poly(ocatedecen-*co*-maleimide) (OMI) (see Figure 6), are viable alternatives for polystyrene as plastic pigments in paper coating as shown in Paper II. Maleimide copolymers have very high glass transition temperatures, 150ºC for OMI and 170ºC for SMI, respectively, and they can be dispersed as spherical nanoparticles with particle size ranging from 50-230 nm in aqueous solution with 20% solids content.

SMI can be prepared either by copolymerization of styrene (S) and maleimide or by direct imidization with primary amines from poly(styrene-*co*-maleic anhydride) (SMA) according to the mechanism presented in Figure 7.[26] OMI can be prepared similarly from the corresponding maleic anhydride, poly(octadecene-*co*-maleic anhydride) (OMA).[27-30] The latter technique of imidization is more favorable than copolymerization and well

studied in literature.[26,31-37] The reactions presented in Figure 7 can occur depending mainly on the reaction temperature. With increasing temperature from 25-120ºC the reaction rate of the reversible ring-opening reaction is increased as well as the irreversible ring-closing conversion improved. Also it has been reported that the higher the molar ratio of primary amine to anhydride, the greater is the ring-closing conversion and the higher the yields of imidization. The fraction of the intermediate compound (b) is insignificant at all temperatures and can thus be neglected.[26] The imidization reaction involves a very high viscous state during the reaction which has been attributed to either intermolar polar association with the half-amide intermediate groups during the ring-opening state or by intermolecular imide formation as described by Moore and Pickelman.[31]

The reaction between anhydride and amine has generally been accomplished in organic solvents, *e.g.* tetrahydrofuran (THF), ethylbenzene (EB), *N,N*-dimethylformamide (NMF) or methyl ethyl ketone (MEK)[26,31-34] or by reactive extrusion as demonstrated by Vermeesch and Groeninckx.[35,36] We synthesized SMI and OMI nanoparticles from corresponding maleic anhydride precursors with ammonia (NH_3) in an organic solvent free process in aqueous phase by thermal imidization at elevated temperature of 150ºC as reported in Paper II. The synthesis will be described in detail in section 3.1.2.

SMA and SMI derivatives have been reported to be used as sizing agents in paper industry[38] but to our knowledge there are no records on OMA or OMI in paper. It is a well known fact that maleimides have a high ability of forming hydrogen bonds which remarkably raises the glass transition temperatures compared to their respective maleic anhydrides (122ºC for OMA and 156 ºC for SMA).[34,36,39] As white, high T_g nanoparticles, SMI and OMI make an interesting candidate for plastic pigment in paper coating. Their performance in paper coating will be evaluated in section 4.2.2.

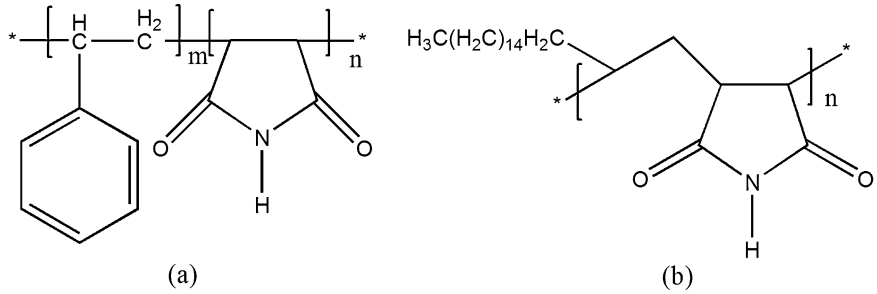

Figure 6: Chemical structures of (a) poly(styrene-co-maleimide) and (b) poly(octadecene-co-maleimide).

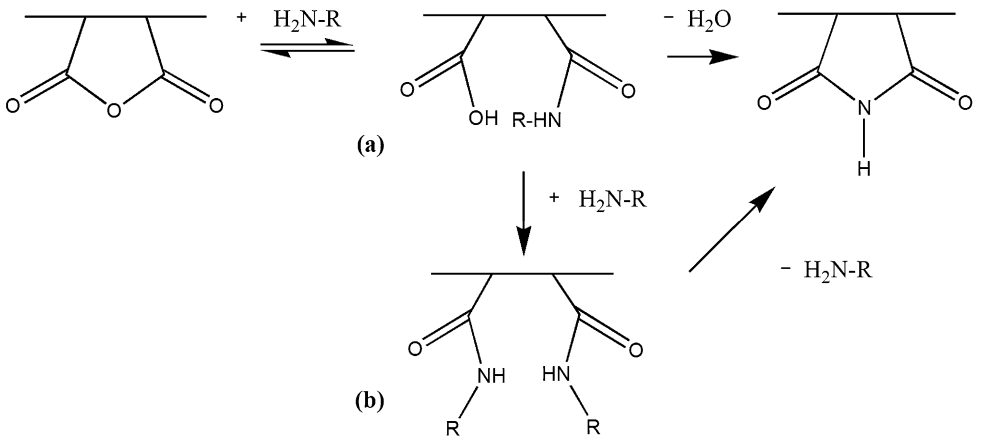

Figure 7: Reaction mechanism of maleic anhydride group to maleimide with intermediate compounds (a) and (b).[26]

Core-shell particles

Core-shell latex is a special type of polymer dispersion where polymer particles comprise a core with one polymer composition covered by a shell with another polymer composition. Thus, the particle properties can be tailor-made for many applications. Via core-shell polymerization also otherwise incompatible monomers can be polymerized into one particle or functionality can be added either into a core or a shell.[40-48] In the core-shell particles, two polymer phases with different refractive indexes are entangled together, thus increasing their light scattering ability compared to solid beads of uniform particle composition.[48]

Core-shell latexes can be prepared by a two-stage emulsion polymerization or seeded emulsion polymerization. In a conventional emulsion polymerization, water-immiscible monomers are emulsified by a surfactant in water and polymerization is activated by a water-soluble free radical initiator resulting in a colloidal dispersion of polymer particles in water. The process can be carried out using batch, semi- or continuous methods. The emulsion polymerization can be divided into particle nucleation and particle growth stages. In the particle nucleation stage, the number of particles formed depends greatly upon the type and concentration of surfactant, the type and concentration of electrolyte, the rate of radical generation and the type and intensity of agitation and temperature. These factors determine the number of particles in the final latex.[49] The emulsion polymerization is a particularly complex system where events occur in both

water and at monomer/polymer sites. In addition to monomers, surfactants and initiator, also different modifiers are involved in the reaction. These components are added to aid and control the polymerization process.[41,43] In a two-stage emulsion polymerization, the core monomers are fed into the reactor allowing them to polymerize first following by the addition of shell monomers. In the seeded emulsion polymerization, the first stage is the preparation of the seed particles. The seeds can be any small particles that can grow to give final latex particles. Typically, seeds are previously prepared latex particles polymerized from monomer with controlled amounts of surfactant and initiator. The seeds are added to the reactor followed by the addition of further monomers. At this point, the nucleation stage is over and particles grow only in size without generating any more new particles allowing better control of particle size and size distribution. The versatility of the seeding process has made it an interesting technique, both from a scientific and an industrial point of view.[45,46,49-54]

In addition to an ideally and clearly divided two-phased core-shell particle structure, several more diffuse morphologies exist. Figure 8 illustrates different core-shell particle formations. The morphology of the particle can change macroscopic properties of the produced material. Both thermodynamic and kinetic properties are the key factors controlling particle morphology.[50,55-62] Landfester *et al.* observed that the reaction temperature affected core-shell interface morphology.[55] Core-shell with a gradient of both compositions is a particularly favorable structure for thermodynamically incompatible polymers.[56] Jönssön *et al.* came to the conclusion that the type of structure obtained depends on the combination of polymerization temperature, the second stage monomer feed rate, the rate of initiation and the seed particle concentration and size.[50] Furthermore, the type and concentration of initiator and emulsifier play a crucial role for resulting morphology.[57-59] Development of the particle morphology is also affected by the diffusion resistance which is related to the chain mobility. The increased internal viscosity during the final stage of polymerization causes restricted chain mobility resulting in a mixture of particles with more than one morphological configuration.[57,58]

Solid core-shell pigments are exceptional in paper coating applications. In Paper I, we prepared a series of plastic pigment core-shell latexes with a soft hydrophilic polymer core of *n*-butylacrylate (BA) and methacrylic acid (MAA) and a hard hydrophobic shell of styrene. The core was partially crosslinked with ethylene glycol dimethacrylate (EGDMA), *N,N*-methylene bisacrylamide (MBA) or 1,1,1-trimethylol propane triacrylate

(TMPTA). During the polymerization, the core was swollen by the addition of sodium hydrogen carbonate ($NaHCO_3$). The particle size of the core-shell latexes varied in a range of 115-285 nm. The synthesis of these core-shell particles is described in section 3.1.1 and their performance in paper coating in section 4.2.1.

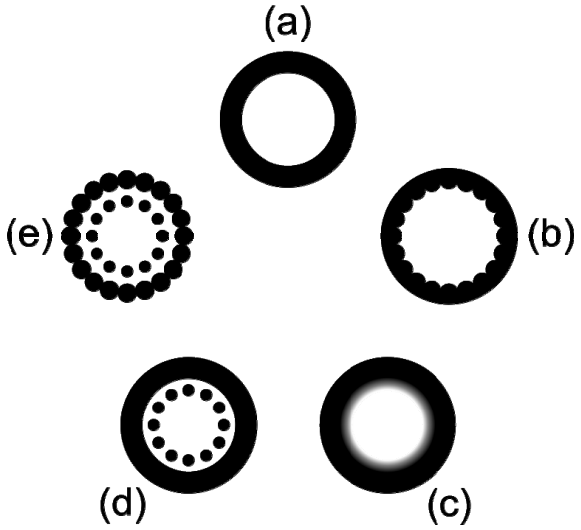

Figure 8: Core-shell particle morphologies: (a) ideal core-shell structure, (b) interface with a wavy structure, (c) interface with a gradient of both components, (d) interface with microdomains, (e) interface of microdomains with an island structured shell. [55]

Hollow spheres

One special group of core-shell latex systems is the so-called hollow spheres that contain a void in their core. The unique flexibility of emulsion processing enables several techniques capable of producing these hollow spheres, *i.e.* osmotic swelling, solvent swelling, incorporation of a blowing agent, water-in-oil-in-water emulsion methods, encapsulation of a non-solvent hydrocarbon and phase separation of two polymers in a solvent.[63-65] Hollow latex particles have proven to be useful in paper coating applications. Due to vast commercial interest in these particles several patents relating to hollow spheres exist, most of them focusing on the osmotic swelling process.[66-68] In this process, the core-shell latex is prepared by a sequential emulsion polymerization. In a subsequent swelling process, water is absorbed into the core and upon evaporation water leaves a void within the particle.[42,64,69] The earliest process for making hollow latex particles via osmotic swelling was developed by Rohm & Haas.[70] Their concept involved making a

structured particle with a carboxylated polymer core. The ionization of the core with a base expands the core by osmotic swelling producing hollow particles with water and polyelectrolyte in the interior. Such core-shell particles are then heated in the presence of a base to a temperature above the softening point of the shell polymer. The base neutralizes the core polymer forming a polyelectrolyte within the particle. The subsequent absorption of water into the interior due to osmotic pressure leads to expansion and void formation. Once expanded the structure must be stable at a broad range of temperatures. The key requirements for hollow particle formation are that the volume of a core must be large enough in order to leave a void upon drying, the shell should have appropriate transport properties for water to penetrate and the shell must have thermoplastic flow properties at the expansion temperature and be sufficiently cohesive and uniform to maintain its integrity.[64,65]

Hollow spheres have substantially the same effects on paper coating as filled solid beads, *i.e.* increased brightness, opacity and gloss, and improved response to calendering resulting in higher bulk. These properties are, if possible, even further enhanced in the case of hollow spheres but due to the complicated production mechanism they are usually more expensive than filled solid beads. With hollow latex particles both particle size and void volume have an impact on paper properties. The brightness and opacity of paper coating formulations containing hollow latex particles increase due to increased light scattering sites in encapsulated air voids within the hollow sphere particles. The presence of voids within the particles also significantly reduces the density of the plastic pigment and contributes to opacity. Furthermore, the voids contribute to the greater response to calendering by making particles more easily deformable in the calender, thus enabling the use of milder calendering conditions. An important note to make about the use of hollow latex particles in paper coatings is the fact that the particle is relatively large, *i.e* the diameter is up to 1 µm and the void is approximately 50% of the particle volume. Since the large portion of the water is contained inside the particle, these latex samples are supplied at relatively low weight solids. The rheology characteristics of these latex samples will be typical of samples with a solids content of double the actual solids which might sometimes cause runnability problems. Obviously, the ultimate impact of hollow latex particles on finished coated paper properties is dependent on several factors such as overall formulation composition, calendering conditions and base paper properties.[1,17,23,65,71]

Modified functional plastic pigments

Plastic pigments can be modified by functional groups in order to give added value and functionality for paper and enabling fine-tuning of coating properties for special applications. In Paper I, a polymerizable optical brightening agent (OBA) was synthesized and incorporated into the core-shell particles. In Paper III maleimide copolymers were modified via *N*-substitution by using primary amines such as triacetonediamine (TAD), aspartic acid (ASP) and fluorinated amines in order to give functionality to coated paper. The chemical structures of the aforementioned functional compounds are represented in Figure 9 and next they will be discussed further.

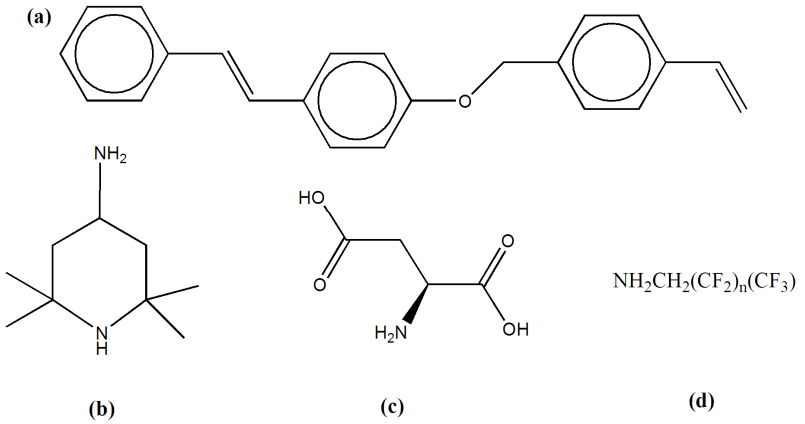

Figure 9: Chemical structures of the modifying compounds: (a) optical brightening agent 1-[(4-vinylphenoxy)methyl]-4-(2-phenylethylenyl)benzene, (b) 4-amino-2,2,6,6,-tetra-mehthylpiperidine (TAD), (c) L(+)-aspartic acid (ASP) and (d) 2,2,2-trifluoroethylamine (TFEA, n=0) and 2,2,3,3,4,4,4-heptafluorobuthylamine (HFBA, n=2).

Optical brightening agents

Optical brightening agents (OBA), also known as fluorescent whitening agents (FWA), absorb UV light in the range of 300-400 nm and radiate the absorbed energy in the blue region of the visible light at 400-450 nm, this phenomenon is known as fluorescence.[72,73] As a result the yellowish tinge of fibers and fillers in paper shifts towards bluish-white thereby increasing the degree of whiteness experienced by the eye. Additionally, brightness is increased by the fact that the eye perceives a larger amount of visible light reflected by the paper than was actually incident on it.[72] Consequently, this leads to sharper contrasts and improved color brilliance in the printed image.[73] OBAs can be added

to paper in paper stock, in sizing or in coating. Already small amounts of OBAs in the coating, 0.8-2.0 parts per hundred (pph) parts dry pigment, are sufficient enough to increase remarkably brightness even up to 15 units. Technically, on the other hand, excess OBA may cause the so-called greening-effect turning the shade of the paper into gray-green therefore the dosage needs to be carefully optimized. The choice and amount of OBA depends on the coating color composition, particularly on the type and amount of co-binder.[74]

The most common OBAs used in the paper industry are stilbene-based derivatives although other types of fluorescent compounds are also available.[73-75] Derivatives of diaminostilbene disulphonic acid (Figure 10) differ in the choice of R_1 and R_2 –groups and the number of sulphonic acid groups, the most common being two, four or six groups.[73,75] The higher the number of sulphonic acid groups, the higher the increased whiteness and brightness but also the price of the compound. Tetrasulphonated derivatives are most sensitive to the greening-effect, nevertheless they account for 80% of the market.[73,74] Another possibility is to synthesize a polymerizable OBA, and thus include this functionality into the plastic pigment thereby reducing the amount of co-binder needed to bind OBA into the coating layer. Most polymerizable OBAs reported are derivatives of *N*-substituted 1,8-naphthalimides (Figure 10).[76-78] In Paper I, a stilbene-based polymerizable OBA, 1-[(4-vinylphenoxy)methyl]-4-(2-phenylethylenyl)benzene (Figure 9), was synthesized. Fluorescence in OBAs originates from relaxation of the electron excitation in the π-bond: in 1,8-naphthalimides it is associated with the transition of carbon-carbon π-bond[79] whereas in stilbenes the π-bond of the *trans*-isomer connecting two phenyl rings accounts for fluorescence.[80]

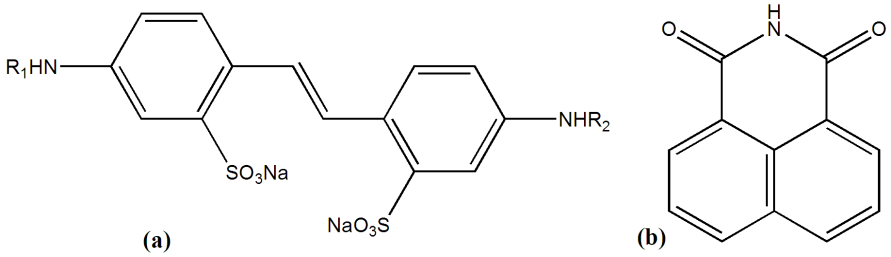

Figure 10: Chemical structure of (a) disulphonated diaminostilbene and (b) 1,8-naphthalimide.

Hindered amine light stabilizers

Synthetic and natural polymers are prone to thermal- and photo-oxidation by a radical-induced process which will lead to undesired changes in physical and visual properties, *i.e.* embrittlement and discoloration.[81] The weathering resistance of polymers can be improved by the addition of the so-called hindered amine light stabilizers (HALS) that are mainly 2,2,6,6,-tetramethylpiperidine, also known as triacetonediamine (TAD), derivatives (Figure 9).[82] Numerous mechanisms of stabilization have been proposed of which the dominating one is the so-called Denisov cycle chain-breaking antioxidant process. According to this mode of action, in the presence of oxygen and UV-radiation an amine in the HALS compound is converted into the corresponding nitroxy radical >NO$^{\bullet}$ which then scavenges a free radical under formation of an aminoether (NOR) that interacts with a peroxide radical under formation of an intermediate structure which finally decomposes into stable non-radical products, such as alcohols and ketones while the nitroxy radical is reformed as depicted in Figure 11.[82-84]

Conventional HALS stabilizers are low-molecular weight compounds that are known to migrate out of the polymer matrix – this can be overcome by using higher molecular weight HALS derivatives or polymeric/reactive HALS that can be chemically tethered to the polymer backbone.[81,85,86] Singh *et al.* have studied a number of polymeric HALS including TAD-*graft*-SMA for stabilizing high impact polystyrene.[81,87,88] In Paper III, the addition of HALS functionality into maleimide particles has been studied.

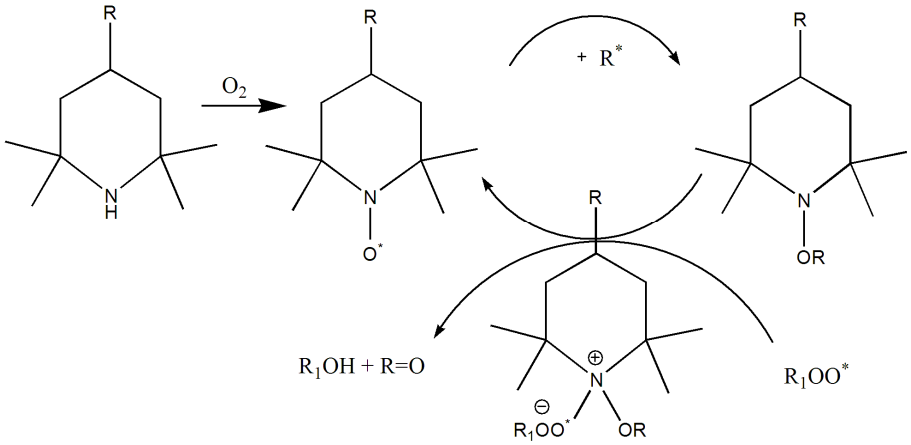

Figure 11: The mechanism of hindered amine light stabilizers (HALS) according to the Denisov cycle.

Aspartic acid

L(+)-aspartic acid (ASP, Figure 9) can be used to control adhesion properties of a material. ASP is widely used in biomedical applications but is rare in the paper industry.[89,90] By incorporating moieties of ASP hydrophilic segments can be introduced into non-polar polymers whereby surface and bulk properties of the host material can be controlled and fine-tuned for the chosen application. Shogren *et al.* have prepared low molecular weight copolymers of ASP by reactive extrusion[91] and Kakuchi *et al.* have successfully reacted ASP with phthalic anhydride.[92] Willet *et al.* studied adhesion of amino acids including ASP to different inorganic surfaces making it possible to regulate adhesive properties of the surface.[93] In Paper III, incorporation of ASP-groups into maleimide copolymers was reported.

Fluorinated compounds

By introducing fluorinated groups into the polymer backbone the surface can be made hydrophobic. Fluorochemicals affect surface tension and thus also the wetting properties of a material. Several reports present successful engineering of maleimide copolymers via attachment of fluorinated side chains providing the desired surface characteristics for various applications.[94-97]

The treatment with fluorochemicals can also be used to improve barrier properties of paper and paperboard. The barrier requirements are typically resistance against water, gas and/or grease. Humidity and moisture weaken the strength of fiber-based materials whereas gas and grease protection is generally required for food packaging. Processes applicable for providing barrier properties are extrusion coating, dispersion coating and sizing, both surface sizing and internal sizing where the barrier compound is added directly to the pulp in the wet end. In extrusion coating polyethylene and ethylene vinyl alcohol copolymers are common barrier materials whereas surface sizing is the general application method for treating paper with fluorochemicals. Unlike polymer films in extrusion coating, fluorochemicals ensure the ability to control the extent of the barrier properties.[98-101] Chemical binding of fluorochemicals to another material, *e.g.* to a coating pigment, diminishes the risks of fluorochemicals migrating out of the paper surface. In Paper III, the effects of incorporation of fluorinated side chains into maleimide plastic pigments were investigated.

2.1.3 Organic-inorganic hybrids

An organic-inorganic hybrid material comprises organic and inorganic components that synergistically combine the properties of the two distinctly dissimilar materials, *i.e.* lightweight, flexibility and good processability of the organic material with high strength, heat stability and chemical resistance characteristic for the inorganic counterpart.[102] Typically, polymers are used as organic phase whereas clay minerals are common inorganic components. Due to their versatility and exceptional properties hybrid materials have been a subject for intensive study and they find applications in a number of fields such as optics, electronics, mechanics, energy, environment, medicine, membranes and coatings.[103]

The three general structures of hybrid materials are illustrated in Figure 12: (1) conventional composites or microcomposites containing tactoids, non-intercalated face-to-face clay layer aggregates, (2) intercalated clay composites where the clay layer spacing has been expanded by the interlayer space intruding molecules and (3) exfoliated composites where the platelets are dispersed as individual units.[104-107] Exfoliated composites are also referred to as polymer-clay nanocomposites (PCN).

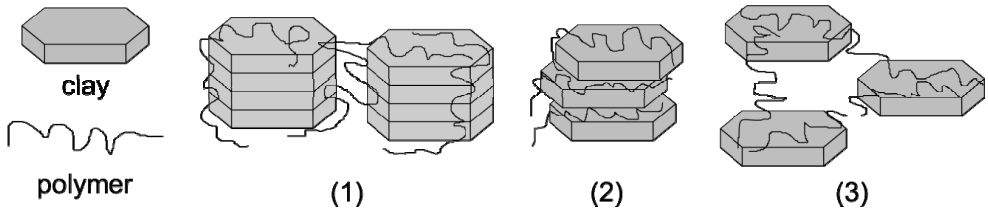

Figure 12: Three general hybrid structures: (1) conventional composites, (2) intercalated composites and (3) exfoliated composites.

Identification of the hybrid structure is generally performed utilizing X-ray diffraction (XRD) technique which gives information on the crystal structure of a material. From the diffraction pattern d-spacing of a crystal can be detected. D-spacing is defined as the distance from a certain plane in one layer to a corresponding plane in another parallel layer of the crystal and thus, in the case of clay hybrids, gives information on the clay layer stacking and material in between the layers. The basal plane (001) represents one atomic layer in the crystal structure. With intercalation an increase in the d-spacing (001)

will be detected and when exfoliated, the clay diffraction peaks disappear entirely because the crystallographic order is lost.[105] Typically, one molecule or more forms a unit cell, the crystal's repeating unit in a crystal lattice. The unit cell, in turn, is divided into planes indicated by coordinates, Miller indexes. Crystallographic planes are categorized in two types of atomic planes: to z-axis perpendicular basal planes and to non-perpendicular prism planes. Some crystal planes found in kaolinite are illustrated in Figure 13. One kaolinite particle consists of approximately 600 unit cells.[108] Before discussing hybrids further, selected inorganic and organic components will be presented in detail in the following sections.

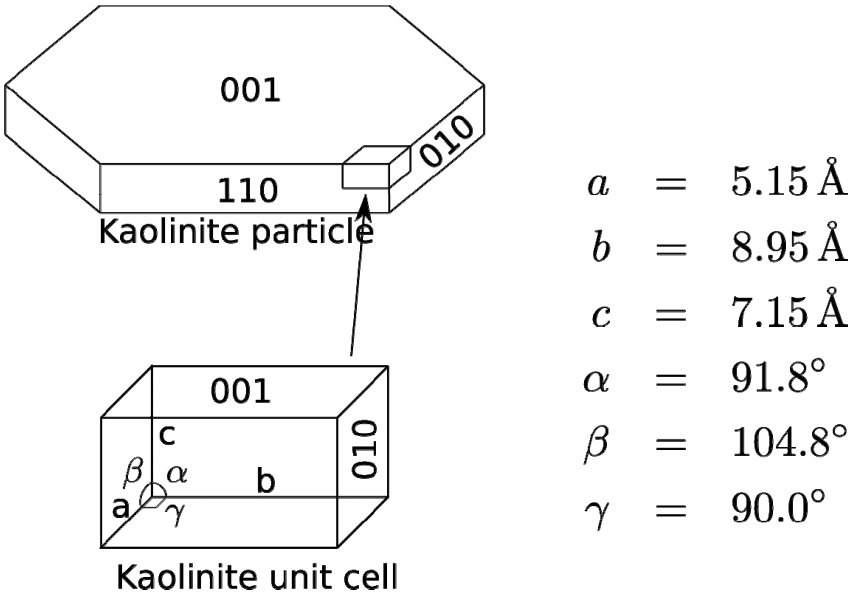

Figure 13: Kaolinite particle and unit cell (triclinic crystal structure) with basal (001) and prism (010 and 110) planes denoted.[108]

Inorganic components

Clay minerals which are phyllosilicates with a layered sheet-like structure generally constitute the inorganic phase of the hybrids. All phyllosilicates comprise tetrahedral and octahedral sheets as their building blocks but depending on their arrangement and composition, phyllosilicates have clearly different physical and chemical properties despite the similarities in their basic structure. The tetrahedron is formed by connecting four oxygen anions surrounding a central cation, predominantly silicon (Si). Correspondingly, the octahedron has oxygen or hydroxyl anions in the corners and an

aluminum (Al), iron (Fe) or magnesium (Mg) cation in the center (Figure 14). Phyllosilicates can have two basic structures: 1:1 layered structure with 1 tetrahedron and 1 octahedron layer and 2:1 layered structure with 2 tetrahedra having 1 octahedron in between them. Kaolinite of the kaolin group phyllosilicates has a 1:1 layered structure whereas montmorillonite of the smectite group constitutes the 2:1 layers.[10,109]

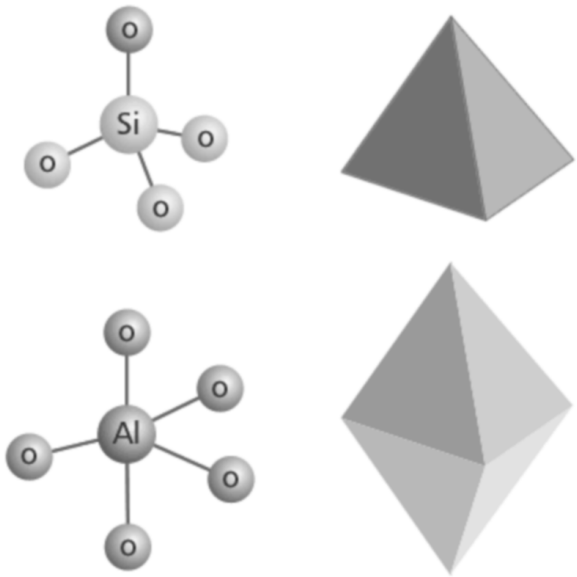

Figure 14: Silica (Si) tetrahedron and aluminum (Al) octahedron structures as building blocks for clay minerals.[10]

Montmorillonite

Montmorillonite (MMT) is one of the most used clay minerals in composite materials due to its excellent intercalation abilities. MMT is a smectite group clay with 2:1 layered structure (Figure 15) defined by oxygen atoms on the edges resulting in a relatively weak interaction between unit cells. MMT is based on a general formula $Al_4Si_8O_{20}(OH)_4$, however some of the aluminum atoms may be replaced by iron or magnesium. MMT has a large cation exchange capacity. In the octahedral sheet, there is a considerable substitution of Fe^{2+} and Mg^{2+} for Al^{3+} that creates a positive charge deficit, thus giving the overall structure a negative charge. These negatively charged layers are held together by charge balancing exchangeable cations such as Na^+ or Ca^{2+} ions. In addition, MMT has a property of holding water molecules between the sheets. Depending on the balancing cation and the

amount of water between the layers, the interlayer spacing can vary from 9.6 to 21.4 Å.[109-111]

Kaolinite

Kaolinite mineral has a chemical composition $Al_4Si_4O_{10}(OH)_8$. Kaolinite, the main constituent in kaolin described in section 2.1.1, has a 1:1 layered structure (Figure 15) defined by hydroxyl groups at one side and oxygen atoms on the other side of a unit cell. There are neither anions nor cations present in the interlayer space but the adjacent layers are linked together by hydrogen bonding.[1,109] Due to this strong interaction, intercalation of kaolinite is more difficult than in smectite type clays in which ions and water are present between the layers and the interlayer bonding is weaker. In addition, cation exchange capacity in kaolinite is considerably lower than in smectite clays. Therefore, studies on kaolinite composites are scarce.[102,108,111-115]

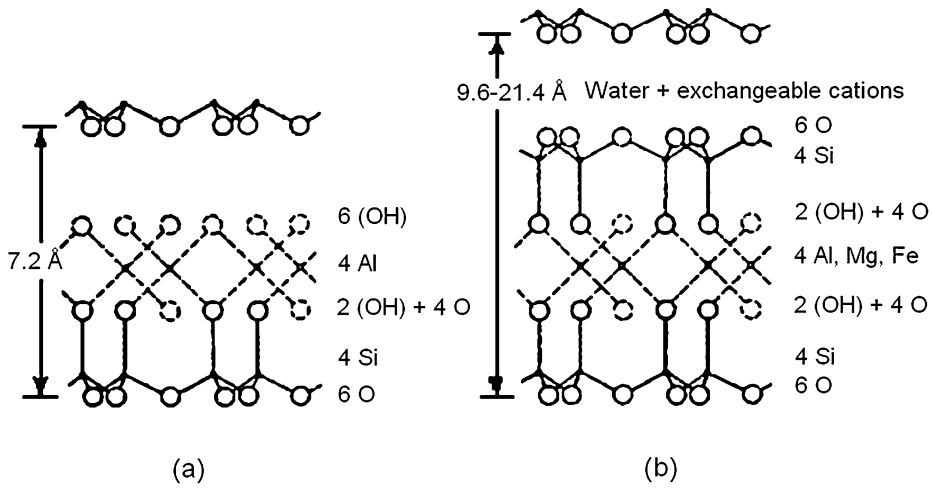

Figure 15: Structures of (a) kaolinite and (b) montmorillonite clay.

Alumina trihydrate

Crystalline aluminum hydroxide, alumina trihydrate (ATH) presented in section 2.1.1, has a chemical formula $Al(OH)_3$. Most ATH is found as mineral gibbsite designated as γ-$Al(OH)_3$. Gibbsite has an aluminum octahedral structure (Figure 14) which is why the structure when occurring in clay is occasionally referred to as the gibbsite layer. In the octahedron, a central aluminum ion is bonded to six octahedrally coordinated hydroxides.

Each of the hydroxides is bonded to two aluminum ions and because one third of the octahedrons are vacant of central aluminum, the result is a neutral sheet. Octahedrons are oriented in such a manner that hydroxide ions of adjacent layers are situated directly opposite each other, thus forming double layers of hydroxide ions. Hydrogen bondings operate between the layers.[15,116-120] Most composite studies on ATH are related to its use as flame retardant filler in plastics.[121,122]

Organic components

Various polymers such as polyamides, polyimides, polyolefins, rubbers, thermoplastic and biodegradable polyesters, styrenic and acrylic polymers, epoxides and polyurethanes have been successfully used as organic matrix.[104,123,124] Hybrids generally improve properties compared to materials made of solely organic or inorganic phase. A number of studies has been made on various polyimide hybrids that show improvements in thermal, mechanical and barrier properties compared to the corresponding pristine polyimide forms.[125-134]

Hybrids

Many reports state that hybrids provide material diversity and afford substantial improvements for instance in mechanical, thermal and gas-barrier properties. In addition, gains in flame and corrosion resistance have been reported for these advanced materials in comparison to traditional materials.[102,104,125,135] In many cases, the most significant improvements in reinforcement and barrier properties have been reported for exfoliated systems or polymer-clay nanocomposites (PCN). In PCNs the reinforcing phase dimensions are of the order of nanometers. Because of the maximal interfacial adhesion due to the nanometer size characteristics, PCNs possess superior properties over the conventional composites.[136,125] The further improved barrier shield, chemical resistance, decreased solvent uptake and reduced flammability of nanocomposites all benefit from hindered diffusion pathways or so-called tortuous path (Figure 16) by increasing the path length that the molecules have to pass while diffusing through the exfoliated structure.[104,126,127,137]

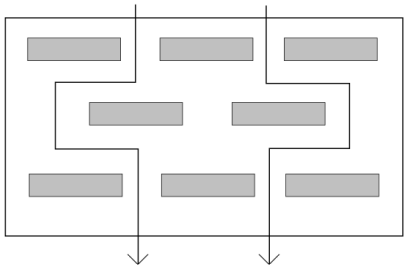

Figure 16: Tortuous path model for enhanced barrier properties of polymer-clay nanocomposites.

Because of the exceptional properties of the nanocomposites, various approaches to enhance the dispersability of these layered plates within the polymer matrix have been of great interest.[104,123] One widely explored strategy to gain better interaction between clay-polymer interfaces in montmorillonite hybrids is to modify the clay surface by treatment with various compounds, such as ammonium surfactants or imidazolium cations with long alkyl tails, thus transforming the hydrophilic, and with the polymer matrix incompatible Na-montmorillonite clay into organophilic montmorillonite or organoclay with increased affinity to the organic phase of the hybrid system by exchanging the sodium cations in the interlayer space with organic cations.[104] In the case of Kaolinite where no ions are present, a so-called guest-displacement method can be exploited where previously intercalated guest organic molecules (*e.g.* dimethyl sulfoxide, DMSO or *N*-methylformamide, NMF) are displaced with the organic polymer matrix[102]. Furthermore, a high shear mixing with much greater forces than those typically reached with a magnetic stirrer are known to improve intercalation and exfoliation.[126] In most of the studies on hybrid materials, clay loadings have been fairly low ranging from 5 ppm up to 10 wt%.[124] Noteworthily, at higher clay contents it is particularly difficult to achieve exfoliation due to strong clay layer interactions.[107]

Most applications of nanocomposites in paper coating are related to improved barrier characteristics although enhancements in other properties such as optical, thermal and mechanical strength and abrasion and scratch resistance are also known.[98] Reinforcing polyamide with clay decreases oxygen transmission rates by half in film extrusion and extrusion coating.[138] On average, commercial nanoclays have aspect ratios from 50 up to 1000 which are much larger than typical clay pigments (10-80) used in paper and paperboard coating.[1,98] Due to the large aspect ratios, nanoclays have high surface area

effectively improving barrier properties even at low concentrations of up to 5 wt%.[98] Nonetheless, a few studies report the use of modified organoclays (montmorillonite and saponite, both from the smectite group) at 5-10 wt% mixed with binder latex (styrene-butadiene and acrylic) and applied on paper coating. In these experiments barrier properties were again tested and improvements even up to four orders of magnitude were reported.[139,140]

Although plastic pigments of large particle size (> 0.5 μm) are known to accumulate on top of the paper due to their light weight, nanosized pigments have a strong tendency of becoming embedded in the pores of the paper substrate thereby rendering them partially ineffective for improving coated paper properties. In Paper IV, a new type of hybrid material was prepared aiming at improving optical and print properties of coated paper. Instead of a continuous polymer matrix, these hybrid pigments consisted of nanosized plastic pigments chemically and physically bound to the inorganic pigment thereby remaining on top of the coating layer for maximal effect (Figure 17). The hybrids were prepared by *in situ* polymerization having poly(styrene-*co*-maleimide) as the organic component and high contents of the inorganic counterpart (70 wt%) of common paper coating pigments, kaolin and/or alumina trihydrate. The synthesis of the hybrids is described in section 3.1.3 and the results of the experiments in paper coating are presented in section 4.2.4.

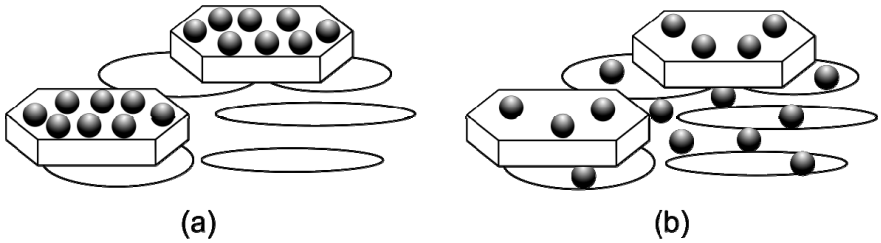

Figure 17: Simplified presentation of (a) organic-inorganic hybrid pigment coating on paper substrate compared to (b) coating with traditional mixture of organic and inorganic pigments.

2.2 Aim of the study

The aim of this research was to prepare new synthetic plastic pigments and hybrids for improving properties of coated paper and paperboard. Since plastic pigments are extensively used in high quality premium paper and paperboard grades where printability and visual properties are of importance, a particular interest of improving these properties existed. Moreover, modification of the new pigments was investigated in order to give functionality to the paper and further develop paper and printing characteristics.

To date, offset printing can be considered to be the dominant method of printing with a market share of over 40%. Offset lithography relies on a simple principle that hydrophobic ink and hydrophilic fountain solution are incompatible and do not mix together (immiscible). Thus, the tacky ink adheres to the image area whereas fountain solution to the non-image area. First, a combination of ink and fountain solution is distributed on a printing cylinder on which the image is created as hydrophobic and oleophilic regions, and then it is transferred to a rubber blanket cylinder that prints the image on paper. In offset printing, the ink splits in the nip whereby a strong perpendicular tack force is imposed on the surface of the paper. These forces cause the paper to climb up the cylinder rolls and may lead to defects such as picking, delamination or blistering. By using functionalized pigments the surface properties of the coated paper can be fine-tuned favorably for the printing process.[1,141,142]

The main objectives of this thesis can be summarized as follows:

- to synthesize and characterize new plastic pigments and hybrids
- to modify plastic pigments in order to give them functionality
- to evaluate the performance of the synthesized pigments in paper coating in laboratory and pilot scale
- to enhance performance and add value of paper and paperboard with new pigments.

3. Experiments

In this chapter, pigment synthesis and applied coating techniques will be described. Additionally, characterization methods of synthetic pigments and papers/paperboards will be presented.

3.1 Synthesis

3.1.1 Synthesis of core-shell latexes

In Paper I reported core-shell plastic pigments were prepared by emulsion polymerization in 1 L jacketed oil heated glass reactor (Figure 18) equipped with a mechanical stirrer (perforated blade), condenser and inlets for addition of chemical. The core consisted of poly(*n*-butylacrylate) (BA) and poly(methacrylic acid) (MAA) and the shell of polystyrene. Furthermore, the core was partially crosslinked with ethylene glycol dimethacrylate (EGDMA) (0.33 wt% of all monomers). In addition, two other crosslinkers were tested: *N,N*-methylene bisacrylamide (MBA) and 1,1,1-trimethylol propane triacrylate (TMPTA). Experiments with polymerizable optical brightening agent 1-[(4-vinylphenoxy)methyl]-4-(2-phenylethylenyl)benzene (1.7 wt% of all monomers) were performed by adding the compound either into the core or shell. In separate flasks, core and shell pre-emulsions consisting of water, surfactant and monomer(s) were prepared under magnetic stirring. First, water and surfactant were added to the glass reactor and mixed at 50 rpm before starting simultaneous feeding of the respective initiator solution and pre-emulsion. The core pre-emulsion was fed into the reactor within 1.5 h and during this time also $NaHCO_3$ was added followed by the addition of shell pre-emulsion, also within 1.5 h. The stirring rate was gradually increased to 200 rpm. The reaction was allowed to continue for an additional hour after all pre-emulsion had been fed into the reaction vessel. Finally, the reaction medium was cooled down, terminated and preservation agents were added.

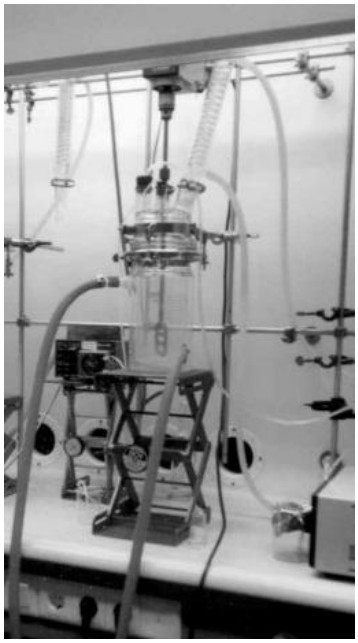

Figure 18: The reactor for core-shell latex synthesis.

3.1.2 Synthesis of maleimide copolymer pigments

Generally, aqueous dispersions of maleimide copolymers and their modifications (Papers II and III) were prepared as follows: in one batch water, ammonia (aq. 25%) and the corresponding maleic anhydride (and modifying compounds) were added into a 1 L autoclave (Büchi, Figure 19) equipped with an anchor stirrer. Mixing was started at the rate of 200 rpm and the reaction vessel was heated with oil bath to 150ºC allowing then the reaction to continue for 5 h. Finally, the reaction was cooled down to room temperature and the resultant polymer dispersion was collected.

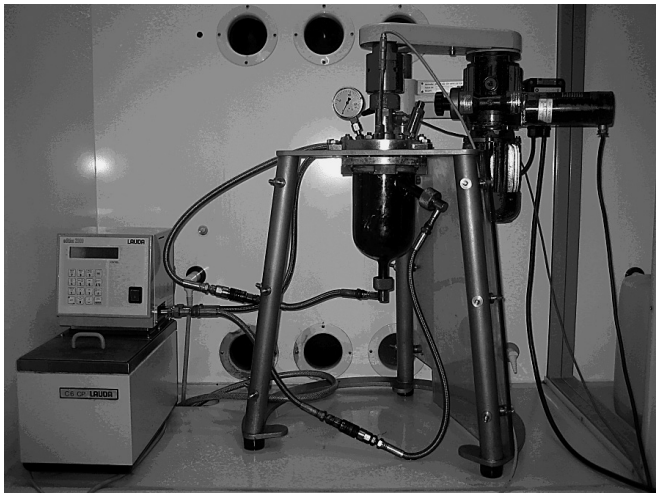

Figure 19: The autoclave for maleimide copolymer and hybrid synthesis.

3.1.3 Synthesis of organic-inorganic hybrids

Aqueous dispersions of organic-inorganic hybrid pigments were also prepared in the autoclave (Figure 19) by an *in situ* polymerization reaction. Poly(styrene-*co*-maleic anhydride) was used as organic precursor and slurries of kaolin (Contour Xtreme from Imerys, UK) and alumina trihydrate (Martigloss from Albemarle, Germany) were used as inorganic phase. Organic and inorganic components together with water and ammonia (aq. 25%) were added in one batch to the reaction vessel. Stirring was started at 200 rpm and the reaction vessel was heated with the oil bath to 160ºC for 6 h before cooling down to room temperature and collecting the hybrid dispersion. Two types of hybrid dispersions with 50% solids content were prepared: 30 wt% poly(styrene-*co*-maleimide)/ 70 wt% kaolin (SMIK) and 30 wt% poly(styrene-*co*-maleimide)/ 35 wt% kaolin/ 35 wt% alumina trihydrate (SMIKA).

3.2 Methods

3.2.1 Coating color preparation

Coating colors were prepared according to the recipes presented in Table 2. The dosage is designated as parts per hundred (pph) parts dry pigment. The components were mixed in the listed order and pH was regulated by sodium hydroxide (NaOH) to 8.5. As a reference a composition without any additional pigment was used consisting of 100 pph main pigment as the sole pigment.

Organic-inorganic hybrids were tested in a simplified coating color consisting of 90 pph Contour Xtreme kaolin as main pigment and 10 pph hybrid sample mixed with 10 pph latex (DOW DL966).

Table 2: Recipes for coating colors

Component	*Dosage (pph)*	*Product name*
Main pigment	100[a]/90[b,c]	Nugloss[a,c]/ Capim NP[b]
Additional pigment	5[a]/10[b,c]	Synthesized pigment
Latex	10	Raisional SB730[a]/ LTX316[b,c]
Thickener	0.5	Finnfix 30 (carboxylmethyl cellulose, CMC)
Calsium stearate	0.6	Raisacoat CAS 50
Hardener	0.2	Raisacoat Az 20 (Azcote)
OBA	0.6	Blancophor B[a]/ Tinopal ABP-Z[b,c]

[a] coating color in Paper I

[b] coating color in Paper II & III for SMI

[c] coating color in Paper II & III for OMI

3.2.2 Coating applications

In Papers I, II and III, coating colors were applied on paper or paperboard using a laboratory scale Helicoater in Raisio, Finland. Coating colors were coated on one side 10 g/m^{2}on a 100 mm wide web. In Paper I, the coating substrate was precoated LWC-paper (light weight coated 39 g/m^2). In Papers II and III, precoated Stromsdal paperboard was used as a coating substrate. The samples were calendered with a laboratory calender and conditioned for 24 h at 23ºC and 50% relative humidity before analysis.

In Paper IV, coating color was applied on paper by a Minilabo Reverse Rotogravure (Yasui Seiki) laboratory coating machine at the Laboratory of Paper Coating and Converting (LPCC) in Turku, Finland. On ground calcium carbonate and kaolin precoated papers (90 g/m^2) a coating amount of 10 g/m^2 on one side on a 100 mm wide web was applied. Samples were conditioned without calendering.

In Paper I, additionally, pilot scale coating and printing trials were performed. Pilot coating was conducted at the Coating Technology Center in Raisio (Forest Pilot Center), Finland and pilot printing at KCL Keskuslaboratorio Centrallaboratorium in Espoo, Finland. A JET-coating machine with IR and air dryers was used in pilot coating applying 10 g/m^2 on both sides of a precoated LWC-paper (38 g/m^2). Coating speed was 1200 m/min and web width 470 mm. Coated paper was then calendered in a nine nip supercalender with a loading of 240-320 kN/m and temperatures ranging from 80-100ºC. Coated and calendered samples were finally printed on a pilot printing machine utilizing the heat set web offset (HSWO) printing technique with all four printing colors (cyan, magenta, yellow and black).

3.2.3 Polymer analysis

Nuclear Magnetic Resonance Spectroscopy (NMR)

In Paper I, the synthesized, polymerizable OBA, 1-[(4-vinylphenoxy)methyl]-4-(2-phenylethylenyl) benzene, was characterized by NMR (Bruker 600 MHz) using benzene-d_6 (C_6D_6) as solvent. Proton (^1H) and carbon (^{13}C) NMR spectra were recorded and chemical shifts (δ) analyzed. In Paper II, ^1H NMR spectrum of poly(octadecene-co-maleimide) dissolved in dichloromethane-d_2 (CD_2Cl_2) was recorded.

Fourier Transform Infrared Spectroscopy (FTIR)

In Papers II and III, the Attenuated total reflection (ATR) – FTIR technique (Sensir Durascope Perkin-Elmer FTIR 1000) was used for collecting IR spectra of maleimide copolymers. In Paper IV powdered hybrids were characterized utilizing the Diffuse reflectance (DRIFT) – FTIR technique (Perkin-Elmer).

Size-Exclusion Chromatography (SEC)

In Paper II, molecular weights (M_w) of maleimide copolymers were determined by SEC (Shimadzu). Polystyrene standard was used for calibration. Samples were dissolved in tetrahydrofuran (THF).

Differential Scanning Calorimetry (DSC)

In Papers II-IV, glass transition temperatures were determined by DSC (TA Instruments DSC Q1000) under nitrogen purge using both traditional and modulated techniques. In the traditional technique, a heating rate of 10ºC/min was used in the temperature range of -50ºC to 200ºC or 300ºC. All data were collected from the second heating round.

Dynamic Light Scattering (DLS)

Particle sizes of dispersions were measured by DLS (Malvern Zetasizer 1000 in Papers I-II and Malvern ZetaSizer Nano ZS in Papers III-IV). The samples were diluted in distilled water and placed in sizing cuvettes illuminated with Helium-Neon laser light. Detection angle adopted in the Malvern Zetasizer 1000 was 90º and in the Malvern ZetaSizer Nano ZS 173º. The average particle diameter was given as an intensity distribution mean value.

Dynamic Surface Tension (DST)

Dynamic surface tension of dispersions in Paper III was determined utilizing maximum bubble pressure method (SensaDyne 9000 Max bubble tensiometer). The tensiometer was calibrated with water and ethanol. Surface tension was registered when the value had stabilized to equilibrium surface tension (σ_{eq}).

X-Ray Diffraction (XRD)

In Paper IV, Wide Angle X-ray diffraction (WXRD, Phillips PW2710) technique with CuKα radiation in the range of scattering angles 2θ of 10º-70º was used for crystal structure analysis of dried hybrid samples. All measurements were taken using a generator voltage of 40 kV and a current of 30 mA.

Electron Microscopy

Electron microscopy techniques, Scanning electron microscopy (SEM) and Transmission electron microscopy (TEM) were used for surface and particle characterization. In Paper I, TEM (JEOL 100SX) image of a core-shell particle was taken. The sample was first dried and then embedded in epoxide followed by a microtomation with a diamond knife into thin layers with a thickness of 20-100 nm. One slice was then chosen and placed on a copper grid for image analysis. In Papers I, II and IV, SEM technique was applied on coated paper surfaces (Cambridge Instruments Stereoscan 360 or Leo Gemini 1530) operating at 2-10 kV. The samples were coated with thin layers of carbon in order to make them conductive.

3.2.4 Coating color and paper analysis

Coating color analysis

The following routine analyses were performed for coating colors: sodium hydroxide (NaOH) consumption, pH, solids content, viscosity (Brookfield and/or HAAKE) and water retention (Åbo Akademi Gravimetric water retention ÅA-GWR).

Paper analysis

Papers and paperboards were analyzed according to valid standards as listed in Table 3. Gloss was measured on a Zehntner ZLR 1050 glossmeter. Optical properties and CIE Lab color values were recorded on an Elrepho (SF 450 in Paper I-III and Datacolor 2000 in Paper IV) spectrophotometer. Accelerated aging in Paper III was performed in a Weiss climate cabinet at 80ºC and 65% relative humidity (RH) for 72 h.

Table 3: Paper and paperboard testing standards

Analysis	*Standard*
Gloss	TAPPI T 480
Opacity	SCAN P 8
Brightness	SCAN P 3
Whiteness	SCAN P 66
Z-strength (Scott Bond)	SCAN P 80
Surface roughness (Parker Print Surf, PPS)	SCAN P 76
Surface strength (IGT)	SCAN P 63
Ink absorption (K&N)	SCAN P 70
Color (CIELAB)	TAPPI T 527
Accelerated aging	ISO 5630-3

4. Results and discussions

In this chapter, the main results obtained in Papers I-IV will be presented and discussed. The chapter is divided into two parts: the first section covers characterization of plastic pigments and the second part their utilization in paper coating.

4.1 Polymer characterization

4.1.1 Core-shell latexes (Paper I)

A series of core-shell latexes with varying compositions (Table 4) were prepared in Paper I. All latexes were stable, uniform and their particle sizes varied in a range of 113-283 nm.

Table 4: Core-shell latex recipes and their particle size

Latex	*S(g)*[a]	*BA(g)*[b]	*MAA(g)*[c]	*Particle size (nm)*
Latex 1	60	20	2	209
Latex 2	60	20	6	113
Latex 3	90	30	6	184
Latex 4	60	40	14	155
Latex 5	75	40	2	275
Latex 6	75	30	14	125
Latex 7	90	30	2	283
Latex 8	90	20	14	166
Latex 9	75	40	10	166
Latex 10	90	20	10	140

[a] The amount of styrene (S) used in shell

[b, c] The amount of *n*-butylacrylate (BA) and methacrylic acid (MAA) used in core

Figure 20 presents a transmission electron microscopy (TEM) image of the core-shell latex. The TEM sample preparation has slightly distorted particles but we can still see darker edges and a lighter center of the core-shell particle in the image. Core-shell structure does not directly represent any of the common morphologies listed in section

2.1.2 in Figure 8. However, it resembles a combination of interface with a wavy structure and interface with a gradient of both components.

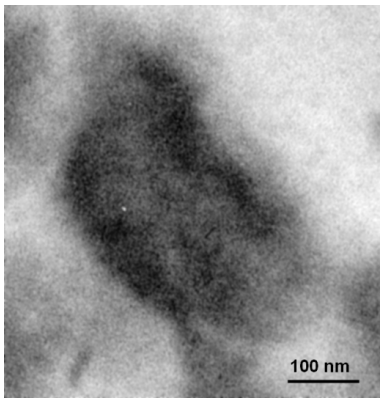

Figure 20: TEM micrograph of core-shell latex particle.

4.1.2 Maleimide copolymers (Papers II-III)

In Paper II, a series of basic experiments were first conducted in order to gain more insight into the effects of different reaction parameters on imidization of maleimide copolymers. It turned out that the best mixing results were achieved with an anchor stirrer using an agitation rate of 200 rpm. A reaction temperature of 150ºC and a reaction time of 5 h were sufficient for the reaction as determined by ATR-FTIR in Figure 21. In the IR spectra the typical doublet peaks of carbonyl groups in anhydride appeared at 1780 and 1850 cm^{-1} and after imidization the peaks had been shifted to 1715 (C=O symmetric stretching) and 1780 cm^{-1} (C=O asymmetric stretching) indicating complete imidization. The conversion of OMI was additionally confirmed by ^{1}H NMR spectra. The peak areas of the methyl group of the bound octadecene at 0.9 ppm were compared to the rest of the bound octadecene at 1.3 ppm and to the peaks of unbound octadecene and 1-octadecene at 5.0-5.8 ppm. Hereby an almost fully imidized OMI was determined with 48.4% bound MI and 48.8% bound octadecene in the polymer.

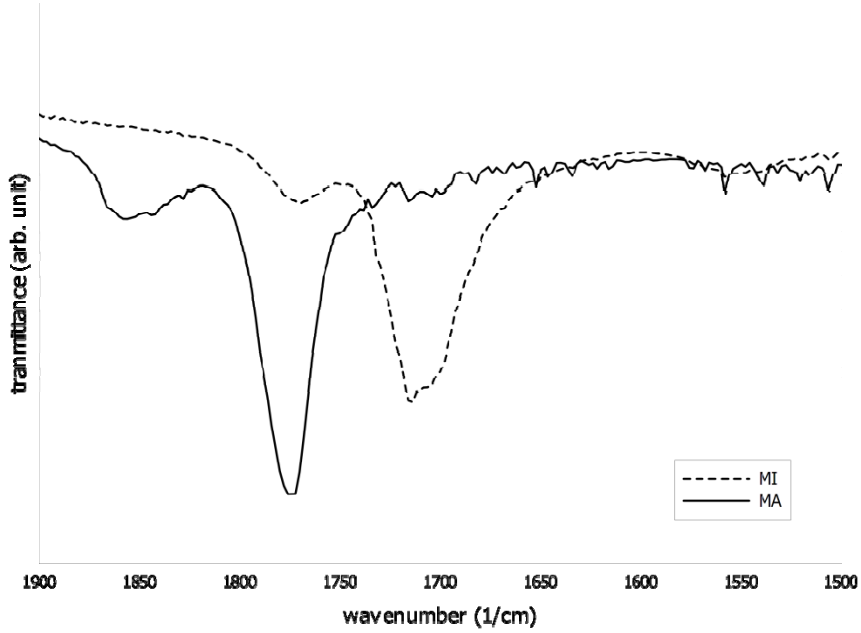

Figure 21: IR spectra of maleic anhydride (MA) and maleimide (MI).

The imidization reaction requires 1 mol of ammonia per 1 mol maleic anhydride unit. The reaction was performed using various molar ratios from 0.5-1.1 thereby producing from completely to partially imidized nanoparticles. The effects of molar ratio were then characterized in terms of glass transition temperature and particle size (Figure 22). T_g:s of the initial anhydrides were 156ºC for SMA and 122ºC for OMA whereas after the imidization, the T_g increased up to 170 ºC and 150ºC, respectively. Glass transition temperatures for SMI are in general higher than for OMI due to the fact that the long aliphatic chain of OMI has much higher mobility than the rigid phenyl moiety in SMI. As expected, T_g increased with increasing fraction of ammonia for both SMI and OMI. The more fully imidized particles, the more hydrogen bonds appear between the particles, which are known to raise T_g. Regarding particle size, with increasing fraction of ammonia, the trend seems to be increasing for SMI and decreasing for OMI. This could be due to the long branches of octadecene which can stretch out and take more volume when there are fewer particles and when they are less densely packed. A molar ratio of 0.95 was finally chosen in order to avoid risk of odor problems due to residual ammonia in the dispersion. The solids content of the prepared dispersions was 20%.

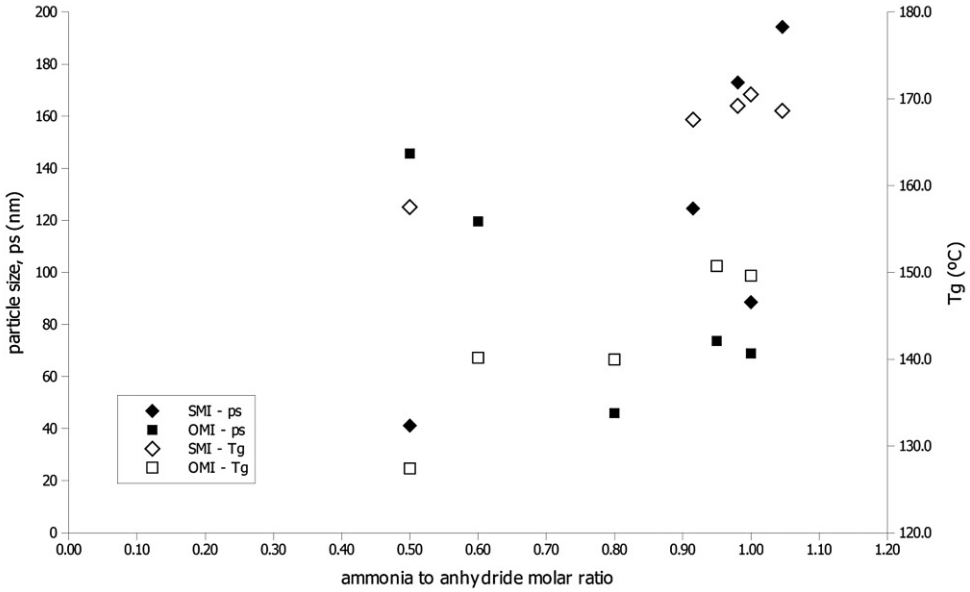

Figure 22: Particle size (ps, filled dots) and glass transition temperature (T_g, hollow dots) as a function of molar ratio of ammonia used in the imidization reaction.

In Paper III, maleimide copolymers were modified by partially replacing small amounts (10 mol%) of ammonia with various functional primary amines, *i.e.* triacetonediamine (TAD), aspartic acid (ASP) and fluorinated amines (2,2,2-trifluoroethylamine, TFEA and 2,2,3,3,4,4,4-heptafluorobuthylamine HFBA), their chemical structures were previously presented in Figure 9. The characteristics of produced modified maleimide dispersions are listed in Table 5. All of the modified maleimide nanoparticles formed stable dispersions, thus the introduction of functional primary amines did not disturb formation of nanoparticles. Additionally, the content of hydrogen bonding was sufficient to ensure high dispersion stability. Particle sizes ranged from 50 to 217 nm and glass transition temperatures varied between 150-180ºC. In general, modifications raised glass transition temperatures and functionalized SMI dispersions had higher T_g values and smaller particle sizes than the corresponding OMI copolymers.

Table 5: Characteristics of modified maleimide copolymers

Sample	*Modifier (wt%)*[a]	*Particle size (nm)*	T_g(ºC)[b]
SMI	-	114	165
SMI-TAD	3.5	71	180
SMI-ASP	3.0	50	176
SMI-TFEA	2.2	87	174
SMI-HFBA	4.4	117	169
OMI	-	69	150
OMI-TAD	1.9	180	148
OMI-ASP	1.6	217	164
OMI-HFBA	2.4	182	NA

[a] Wt% modifier of total solids

[b] Glass transition temperature

Modified maleimide copolymers were characterized by ATR-FTIR. The spectra for modified and unmodified OMI are depicted in Figure 23. In the spectrum of all modifications, the characteristic imide peaks at 1715 and 1780 cm^{-1} can be found and the anhydride peak at 1850 cm^{-1} is either missing or very small. In OMI-ASP spectrum, the fairly strong peak at 1770 cm^{-1} can be attributed to succinic acid end groups. The presence of perfluoroalkyl in OMI-HFBA is indicated by a new peak at 1220 cm^{-1} (CF_3 stretching). Maleimide dispersions modified with HFBA were further analyzed with a bubble tensiometer for determining surface tensions. As expected, fluorination decreased surface tensions even though the decrease was fairly small in the case of OMI. This can partially be attributed to the relatively low concentration of HFBA units in modified OMI. The unmodified SMI and SMI-HFBA possessed surface tension values of 84 and 74 mN/m, respectively. In the case of OMI, only a slight decrease in the surface tension could be detected, from 70 mN/m for unmodified OMI to 69 mN/m for OMI-HFBA.

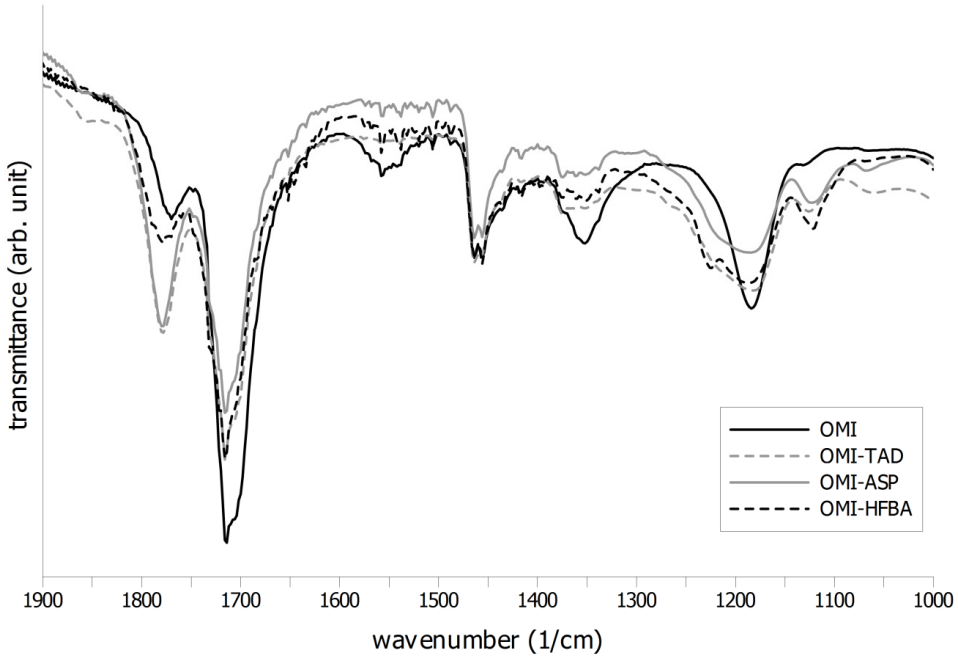

Figure 23: IR spectra of N-substituted poly(octadecene-co-maleimide).

4.1.3 Organic-inorganic hybrids (Paper IV)

Hybrid pigments and their inorganic constituents were characterized by DRFIT-FTIR and XRD in Paper IV. In the IR spectra in Figure 24 for kaolin (K), all four characteristic OH stretching peaks at 3696, 3669, 3653 and 3621 cm^{-1} were found. Alumina trihydrate (ATH) on the other hand exhibited OH stretching bands at 3656, 3621, 3527, 3462 and 3397 cm^{-1}. In the hybrids spectra, new peaks appeared around 3000 cm^{-1} which is typical for polystyrene structure. Also, the formation of maleimide in the hybrids was confirmed by the appearance of the characteristic double peak at 1715 and 1780 cm^{-1}. Additionally, in poly(styrene-*co*-maleimide)/kaolin hybrid (SMIK) a very broad shoulder at 3450 cm^{-1} was detected which is assigned to hydrogen-bonded NH-groups whereas in poly(styrene-*co*-maleimide)/kaolin/alumina trihydrate hybrid (SMIKA) this region is overlapping with the OH stretching bands of ATH. Furthermore, the recorded decreases of intensities of the peaks at 3696 cm^{-1} for the hybrids compared to the kaolin spectrum support the existence of H-bonding.

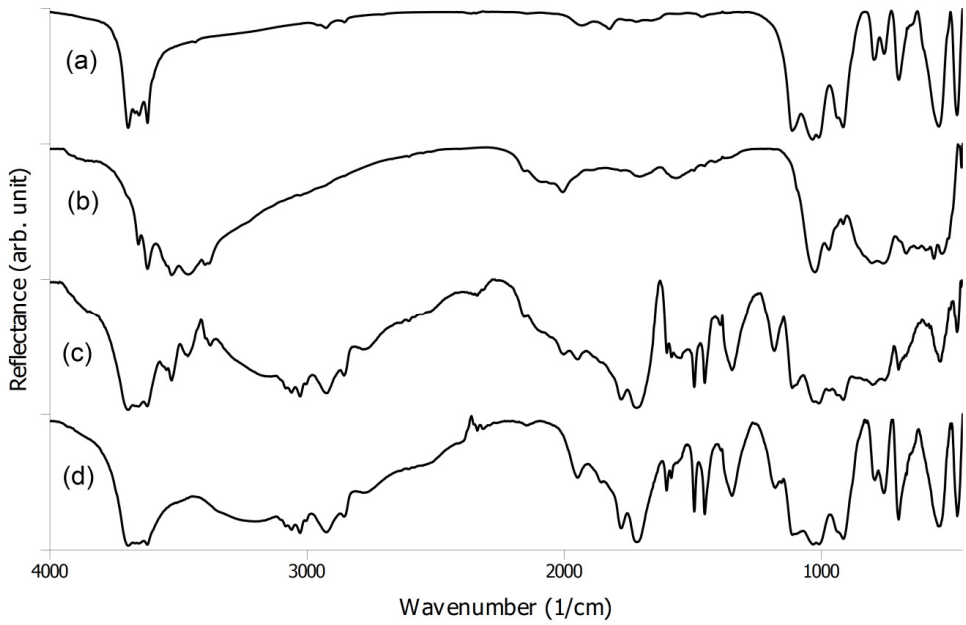

Figure 24: DRIFT-FTIR spectra: (a) kaolin (K), (b) alumina trihydrate (ATH), (c) poly(styrene-co-maleimide)/kaolin/alumina trihydrate hybrid (SMIKA) and (d) poly(styrene-co-maleimide)/kaolin hybrid (SMIK).

Figure 25 shows the XRD diffraction patterns of the analyzed hybrids and their inorganic components over the 2θ range 10-30º. Kaolin had two strong peaks at 12.4º and 24.9º which correspond to basal planes (001) and (002) with d-spacings of d_{001} 7.1 Å and d_{002} 3.6 Å, respectively. For the hybrids SMIK and SMIKA these basal plane peaks appeared in the same region, thus with the same d-spacings, indicating that no intercalation or exfoliation took place. Moreover, a third small peak at 19.9º corresponds to the prismatic cell plane (020) perpendicular to basal plane with d-spacing d_{020} 4.5 Å. For SMIK this peak appears equally at 19.9º, whereas for SMIKA it appears at 18.4º which may be due to the interference of the ATH peak at 18.3º, both with a d-spacing of 4.8Å. ATH gave additionally a strong peak at 20.3º with a d-spacing of 4.4Å which was equal for SMIKA. Thus, we can confirm that the hybrids had a conventional composite structure with aggregates of inorganic components and no exfoliation or intercalation occurred.

Hybrid dispersions had solids content of 50%. Poly(styrene-*co*-maleimide)/kaolin (SMIK) had glass transition temperature of 178ºC and poly(styrene-*co*-maleimide)/ kaolin/alumina trihydrate (SMIKA) 181ºC. Their bimodal particle sizes were 92 and 882 nm for SMIK and 65 and 785 nm for SMIKA where the first value is assigned to

polymer particles and the second to the inorganic components. Particle sizes for components solely were 487 nm for kaolin, 552 nm for alumina trihydrate and 111 nm for SMI, respectively. Hereby, the imidization in the presence of inorganic particles has resulted in decreased polymer particle size and increased inorganic particle size, thus indicating attachment of polymer particles to the inorganic particles. These results should however be considered as indicative because the dynamic light scattering technique is primary designed for spherical monodispersed samples.

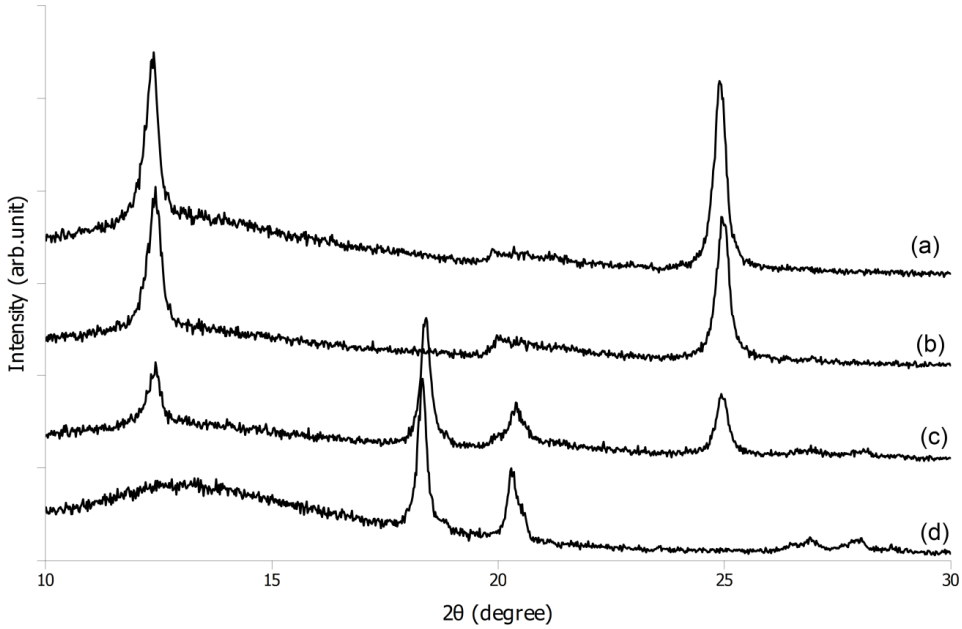

Figure 25: XRD diffraction patterns: (a) kaolin (K), (b) poly(styrene-co-maleimide)/kaolin hybrid (SMIK), (c) poly(styrene-co-maleimide)/kaolin/alumina trihydrate hybrid (SMIKA) and (d) alumina trihydrate (ATH).

4.2 Effect of synthetic pigments on paper coating

The prepared synthetic pigments were coated on paper with a laboratory scale coater in Papers I-IV. Additionally, a pilot scale coating was performed in Paper I. These results will be presented in the following sections.

4.2.1 Effect of core-shell pigments (Paper I)

Laboratory scale trials

In Paper I, coating colors were successfully mixed from 10 selected core-shell pigments and compared to a reference without any additional pigment in Helicoater laboratory coating trials. For most of the core-shell dispersion formulations, as can be seen in Figure 26, improvements in gloss, IGT and surface roughness were achieved compared to the reference. The IGT test measures the ability of a coated surface to resist picking or blistering during offset printing. The measurement is conducted with IGT laboratory printing device. It is generally known that gloss of coated paper is greatly dependent on surface smoothness: the smoother the surface the higher the gloss. In this case, however, the recorded surface roughness values did not fully correlate with the gloss values. Therefore, the effects of other parameters also on the development of gloss were investigated. When comparing latex compositions in Table 4 and gloss values in Figure 26, a similar trend of increasing gloss with increasing fraction of styrene units as reported by Taber *et al.*[4] for styrene-butadiene latexes could be detected also for core-shell latexes. Furthermore, the gloss increased with decreasing fraction of butyl acrylate units. Consequently, having a high fraction of styrene and a low fraction of butyl acrylate in the core-shell latex had a beneficial impact on the paper gloss.

Next, the type of crosslinker used was studied in terms of various paper properties listed in Table 6. The following three crosslinkers were tested: ethylene glycol dimethacrylate (EGDMA), *N,N*-methylene bisacrylamide (MBA) and 1,1,1-trimethylol propane triacrylate (TMPTA). The best gloss, brightness and smoothest surface were achieved with EGDMA while the surface strength was weakest for EGDMA. TMPTA had the lowest gloss whereas MBA had the roughest surface. In general, EGDMA seemed to exhibit the best balance of properties and was therefore chosen as the candidate for further testing in pilot trials.

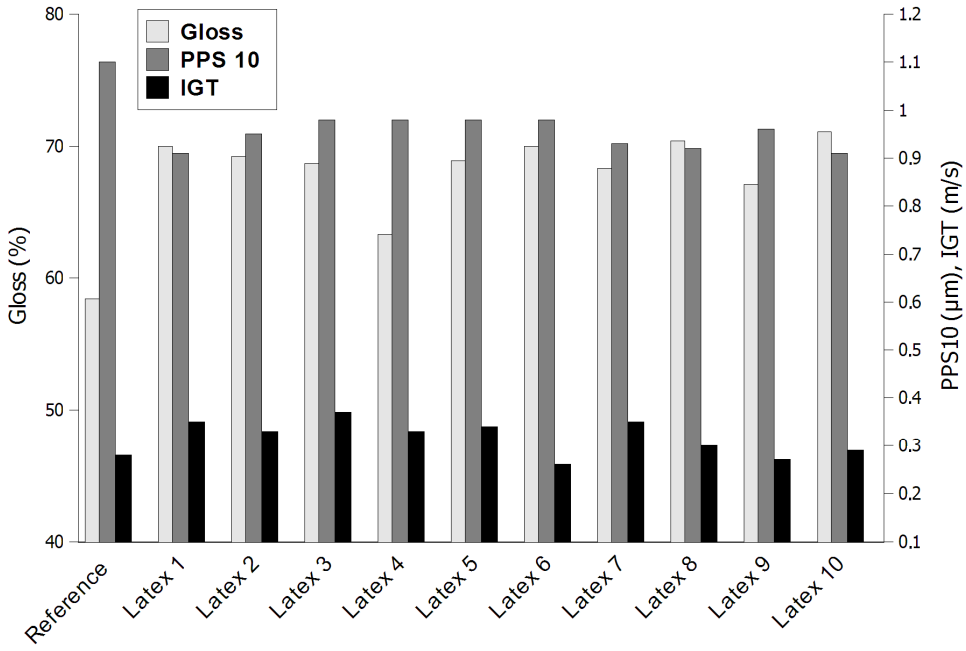

Figure 26: Gloss, PPS10 surface roughness and IGT surface strength of paper samples coated with core-shell latexes.

Table 6: Effect of different crosslinkers in core-shell latex on paper properties

Crosslinker	*Gloss (%)*	*PPS10 (µm)*	*K&N*	*IGT(m/s)*	*Brightness (%)*
EGDMA	61.20	1.20	12.1	0.14	75.9
MBA	60.30	1.40	11.1	0.17	69.2
TMPTA	56.80	1.27	12.3	0.17	69.9

Pilot scale trials

Latex 10 with its most promising combination of properties was chosen as a candidate for further studies and after minor modifications (using 2 g of MAA instead of 10 g, and 0.6 g of surfactant instead of 0.4 g) it was upscaled to 200 L. The new latex was denoted as Scaleup 10 and used for pilot coating and printing trials. Coating colors were prepared in two concentrations, *i.e.* 4 pph and 8 pph (parts in respect to 100 parts of main pigment by weight) and a solid content of 55%. As a reference a coating without any additional

pigment was used. Figure 27 shows SEM images of samples from the pilot coating trials. The first image (a) contains no additional latex whereas the second one (b) contains 8 pph core-shell latex Scaleup 10. Kaolin particles of > 1 µm in diameter can be found in both images. Spherical core-shell latex particles seen in the second image (b) are approximately 290 nm in diameter. The pilot trials proceeded smoothly and the overall runnability was excellent. Z-strength (Scott Bond), PPS surface roughness, gloss, mottling, print through and print density were analyzed. Some of the results are listed in Table 7. Z-strength was reduced compared to the reference when 4 pph Scaleup 10 was added whereas it increased in the case of 8 pph of the same. PPS and print gloss were improved for both concentrations, but for these parameters the improvements were greater for lower concentration of Scaleup 10. The reduction in print gloss with increasing concentration from 4 pph to 8 pph could be partially attributed to its rougher surface, *i.e.* the higher particle concentration cannot any more even out the surface. The optimal concentration of the core-shell latex is therefore dependent on the desired effects.

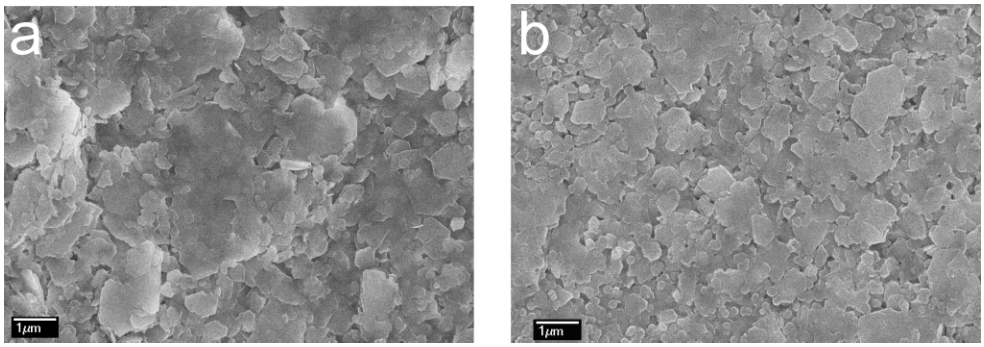

Figure 27: SEM images of coated and calendered pilot trial papers (a) without core-shell latex particles and (b) with 8 pph Scaleup 10.

Table 7: Some characteristics of paper samples retrieved from pilot trials

Sample	*Z-strength (J/m²)[a]*	*PPS 10 (µm)[b]*	*Print gloss (%)[b]*
Reference	346	1.90	63.8
Scaleup 10 (4 pph)	341	1.74	66.6
Scaleup 10 (8 pph)	354	1.81	65.5

[a] After pilot coating and calendering

[b] After pilot printing from four color black

Effect of polymerizable optical brightening agent

The next development of core-shell latex Scaleup 10 was the inclusion of polymerizable optical brightening agent 1-[(4-vinylphenoxy)methyl]-4-(2-phenylethylenyl)benzene either into the core (Optiscaleup 1) or into the shell (Optiscaleup 2). The coating trials were performed on the Helicoater laboratory scale coater. Figure 28 demonstrates the effect of polymerizable OBA in the core-shell latex on paper gloss and brightness. As expected, brightness increased from 68.4% to 69.3% with OBA in the core and to 69.2% with OBA in the shell. Even though the increase was not exceedingly remarkable, it proved the effect of optical brightening agent. OBA had the same effect both in the core and in the shell. Additionally, gloss was increased from 62.9% to 66.8% and 65.8% for Optiscaleup 1 and Optiscaleup 2, respectively. Furthermore, the surface roughness decreased from 1.15 µm to 1.05 µm for core-shell latexes with OBA. The results indicate that the addition of polymerizable OBA can further enhance paper properties. Moreover, migration of OBA from the paper surface is hindered by chemical attachment to the core-shell latex particles.

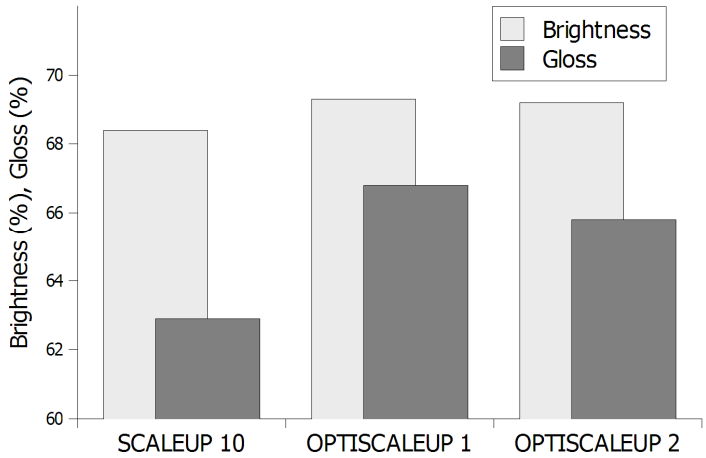

Figure 28: The effect of polymerizable optical brightening agent in core-shell latex on paper gloss and brightness.

4.2.2 Effect of maleimide copolymers (Paper II)

In Paper II, plastic pigments of poly(styrene-*co*-maleimide) (SMI 10-0) and poly(octadecene-*co*-maleimide) (OMI 1-1) were tested on paperboard in Helicoater laboratory coating trials. In coating color formulations delaminated grades of Capim NP and Nugloss were added as main pigment with SMI and OMI, respectively. As references coating colors containing the aforementioned main pigments as the sole pigment were used.

Coating colors prepared from the plastic pigment dispersions had lower viscosities (Br 100) and water retention values (ÅA-GWR) than the references (Table 8). This could be attributed to a difference in the particle size and shape of the pigments. Thus, spherical and hard organic nanopigments with a diameter of 50-100 nm contributed less to the increase of coating color viscosity and water retention values than pseudo-hexagonal platy kaolin pigments with a diameter of > 1 µm. In general, these plastic pigment containing coating colors had good flow properties and runnability.

The SEM micrographs of coated and calendered paperboards containing SMI and OMI in Figure 29 show discrete spherical particles. Thus, the synthesized hard and thermally resistant polymeric nanoparticles survived the calendering process without further deformation, and SMI with higher T_g seems to be even more intact than OMI. SEM pictures also reveal that these small particles tend to penetrate into the porous paper coating structure. Consequently, some of the desired effects of improved surface properties were slightly hampered by the fact that nanopigments were partially imbedded into the porous paper matrix. Therefore, paper properties such as gloss and PPS surface roughness were impaired for samples containing the synthetic pigments. On the other hand, brightness, K&N-ink absorption and IGT pick were improved for these coatings. The results are summarized in Table 8.

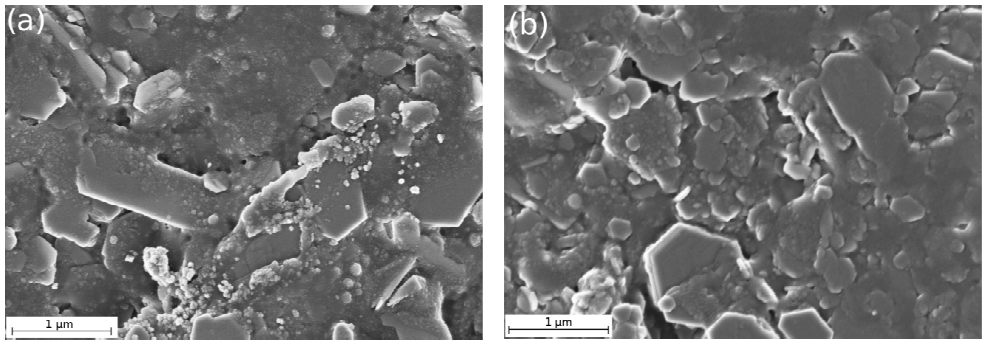

Figure 29: SEM micrographs of paperboard coated with (a) SMI and (b) OMI.

Table 8: Results from coating trials with maleimide copolymers as additional pigment

Sample	*Primary pigment*	*Additional pigment*	*ÅA-GWR (g/m^2)*	*Br 100 (Pas)*	*Gloss (%)*	*PPS 10 (µm)*	*Brightness D65 (%)*	*K&N (%)*	*IGT pick (m/s)*
Ref 1[a]	CapimNP (100pph)	-	56	213	53	1.7	89	5.9	1.3
SMI	CapimNP (90pph)	SMI 10-0 (10pph)	24	172	35	2.0	91	1.8	1.8
Ref 2[b]	Nugloss (100pph)	-	101	185	43	1.9	87	7.4	1.7
OMI	Nugloss (90pph)	OMI 1-1 (10pph)	55	154	39	2.4	89	5.5	3.9

[a] Reference for SMI

[b] Reference for OMI

4.2.3 Effect of modified maleimide copolymers (Paper III)

In Paper III, maleimide nanopigments were modified with hindered amine light stabilizer (HALS), aspartic acid (ASP) and fluorinated compounds (TFEA, HFBA) and applied on paperboard in Helicoater laboratory scale coating trials.

Dewatering of a coating color is a function of base paper, coating properties and particle interactions. It affects not only process runnability and drying of the coating layer but also physical properties of the coated paper and final print quality. Certain coating techniques, such as applicator roll coating, benefit from greater dewatering whereas in blade coating this is generally considered as a problem. Excess dewatering causes a drastic

increase in solid content and thereby hinders runnability of the process.[1,143] ÅA-GWR is used for measuring dewatering of coating color and it is based on a gravimetric method. High dewatering leads to low water retention, *i.e.* the water-holding property of the coating color. As listed in Table 9, all of the modified maleimide pigments increased water retention of the coating color in comparison to the reference containing only main pigment. Furthermore, the measured viscosities of the coating colors with modified nanoparticles were in the range of good flow properties resulting in excellent runnability.

Surface roughness of the coated and calendered paperboards were somewhat increased and gloss was reduced. On the other hand, brightness, K&N ink absorption and IGT pick were all slightly improved (Table 9). As could be anticipated, maleimide nanopigments modified with ASP had the lowest IGT pick values which could be either a result of decreased coating cohesion or strong ink-coating adhesion. Furthermore, K&N ink absorption was lowest for the hydrophobic fluorinated maleimide nanopigments. This result is also in line with earlier findings which have shown that paper treated with fluorochemicals have high repellent characteristics towards other organic compounds such as grease/oil and exhibit improved barrier properties.

The impact of triacetonediamine (TAD) on weathering was tested in a climate cabinet at 80ºC and 65% relative humidity for 72h according to a so-called moist method of accelerated aging (ISO 5630-3). Three days of weathering at 105ºC alone (ISO 5630-1) corresponds to 25 years of natural ageing but does not take into account the presence of environmental humidity, and this omission has led to the development of the moist method.[144] The results of the moist method show almost constant decrease in CIE whiteness despite the presence of hindered amine light stabilizer TAD. Whiteness of SMI drops down from 99.3 to 77.6 and of SMI-TAD from 99.0 to 77.4 thus the total whiteness drop in SMI and SMI-TAD were 21.7 and 21.6 units, respectively. Consequently, the desired improvement in weathering stability was not achieved by this modification. The lack of improved light stability in terms of CIE whiteness can be at least partially attributed to the fact that the stabilizer may not be present in a sufficient concentration in the right phase and at a reasonable depth. In addition, it has been shown that polymeric TAD additives show low activity in polymers that have a high degree of hydrogen bonding. This is explained by the fact that N-H group forms intramolecular hydrogen bonds that prevents its conversion to the active nitroxyl radicals ($NO^{\bullet}$) which in turn is necessary for stabilization of polymers, as demonstrated in Figure 11.[87]

Table 9: Results (before aging) from coating trials with modified maleimide copolymers

Sample	*ÅA-GWR* (g/m^2)	*Br 100* (*Pas*)	*Gloss* (%)	*PPS 10* (µm)	*Brightness D65* (%)	*K&N* (%)	*IGT pick* (m/s)
Ref 1[a]	56	213	53	1.7	89.2	5.9	1.3
SMI[a]	24	172	35	2.0	91.0	1.8	1.8
SMI-TAD[a]	36	170	39	2.2	90.4	1.7	1.8
SMI-ASP[a]	21	172	44	2.2	90.3	1.8	1.3
SMI-TFEA[a]	33	163	41	2.2	90.0	1.3	1.8
Ref 2[b]	101	185	43	1.9	87.0	7.4	1.7
OMI[b]	55	154	39	2.4	89.3	5.5	4.0
OMI-TAD[b]	88	244	29	2.0	88.6	2.4	2.6
OMI-ASP[b]	98	247	49	1.3	84.8	2.0	2.1
OMI-HFBA[b]	96	225	38	2.0	88.4	0.7	2.9

[a] Primary pigment Capim NP

[b] Primary pigment Nugloss

4.2.4 Effect of organic-inorganic hybrids (Paper IV)

In Paper IV, the synthesized hybrid pigments SMIK (poly(styrene-*co*-maleimide)/kaolin hybrid) and SMIKA (poly(styrene-*co*-maleimide)/kaolin/alumina trihydrate hybrid) were tested in paper coating on a Minilabo Reverse Rotogravure (Yasui Seiki) laboratory scale coating machine. In order to study how these hybrid particles act as additional pigment on paper, a simplified coating color formulation consisting of 90 pph primary pigment (Imerys Contour Xtreme), 10 pph hybrid and 10 pph binder latex (DOW DL966) was utilized. The reference contained 100 pph primary pigment. Viscosities of the coating colors were extremely low (< 100 Pas measured by Brookfield 100) because no thickeners were added. Paper analysis is summarized in Table 10. Results show an increase in gloss in all samples containing additional pigments. The increase is greatest for the pure plastic pigment SMI even though it also has the roughest surface. Surface roughness is almost the same for Ref, SMIK and SMIKA, thus the presence of plastic pigments attached to the inorganic pigments in hybrids has not increased the surface roughness.

Scanning electron microscopy images of the coated paper samples in Figure 30 give an insight into the location of discrete spherical nanoparticles in the coating structure. Plastic pigments are seemingly more spread out on the surface when they are combined in hybrids than when they are used as sole additional pigments. Particularly in SMIKA, the plastic pigments seem to have covered entirely some of the hexagonal inorganic particles. Brightness and whiteness was decreased for plastic pigment alone but the difference was only minor in the hybrids compared to the reference. Unfortunately, no whiteness increase was detected when employing an extremely high whiteness pigment, alumina trihydrate, as part of the hybrid. This could be due to the high coverage of ATH pigments by plastic pigments. Opacity of the papers was not significantly affected by the addition of hybrid pigments.

In addition to gloss increase, another further benefit of the hybrids is that they are less likely to form dust during application in comparison to a normal blend of nanopigments in paper coating. The health issues of nanoparticles are one concern surrounding the nanotechnology today. Thus, this method provides a practical approach for dispersing nanoparticles and binding them onto the inorganic surfaces preventing migration and dusting in such a manner that the hybrid pigments can be utilized for improving paper coating properties.

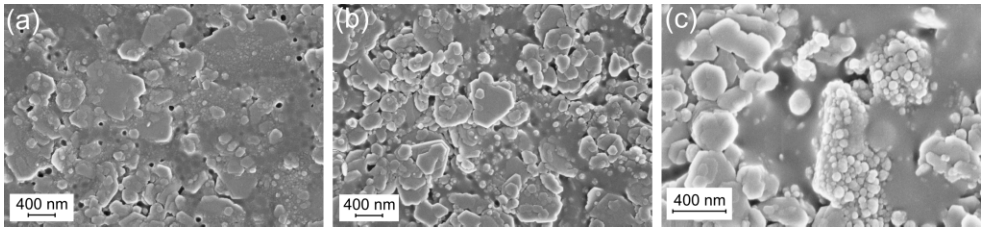

Figure 30: SEM micrographs of paper coated with (a) (poly(styrene-co-maleimide)(SMI) (b) (poly(styrene-co-maleimide)/kaolin hybrid (SMIK) and (c) (poly(styrene-co-maleimide)/ kaolin/alumina trihydrate hybrid (SMIKA).

Table 10: Results from analysis of papers coated with hybrid pigments

Sample	*Gloss (%)*	*PPS 10 (µm)*	*Brightness D65 (%)*	*Whiteness D65 (%)*	*Opacity (%)*
Ref [a]	64.6	1.24	81.8	80.6	96.8
SMI	69.9	1.57	79.0	76.5	96.0
SMIK	67.1	1.21	81.1	80.2	96.5
SMIKA	65.8	1.22	81.2	80.1	96.8

[a] 100 pph primary pigment Contour Xtreme

5. Conclusions

New plastic pigments were successfully synthesized in this work and applied in paper and paperboard coating as additional pigments. We were able to determine some of the plastic pigment characteristics affecting gloss development. High styrene concentration and low butyl acrylate concentration in core-shell latexes resulted in increased paper gloss. Furthermore, the choice of cross-linker in partially crosslinked core-shell latexes affected paper characteristics. The best overall performance was achieved by ethylene glycol dimethacrylate (EGDMA). Additionally, the core-shell latex was successfully modified by the incorporation of a new polymerizable optical brightening agent (OBA) 1-[(4-vinylphenoxy)methyl]-4-(2-phenylethylenyl)benzene for further enhancing paper properties. Moreover, the synthesized core-shell plastic pigments performed well in pilot scale trials.

Plastic pigments based on maleimide copolymers, poly(styrene-*co*-maleimide) (SMI) and poly(octadecene-*co*-maleimide) (OMI), were intensively studied. The effect of different reaction parameters was possible to define and determine the optimal reaction conditions for the synthesis. The prepared SMI and OMI dispersions were also utilized in paper coating. Nanosized particles were partly imbedded into the porous paper structure, however improvements in brightness, K&N ink absorption and IGT pick in comparison to the reference could still be detected. We foresee a great potential in these maleimide nanoparticles due to their versatility, hardness and high thermal stability.

Functionalization of the maleimide copolymers SMI and OMI was performed using triacetonediamine (TAD), aspartic acid (ASP) and fluorinated compounds (TFEA, HFBA) through a thermal imidization reaction. The syntheses were successful and resulted in stable dispersions. The modified copolymers were applied in paperboard coating. Fluorinated groups and aspartic acid modified nanoparticles showed, expectedly, changes in surface properties of the coated paperboard whereas no significant improvements in light stability were achieved with TAD modified copolymers. Additionally, all prepared plastic pigments had good runnability in the coating process.

Organic-inorganic hybrids of 30 wt% poly(styrene-*co*-maleimide) and high levels of 70 wt% inorganic components, kaolin and alumina trihydrate, were prepared by an *in situ* polymerization method. The hybrids had a conventional composite structure with inorganic components covered with precipitated SMI nanoparticles attached to the surface

via hydrogen bonding. In paper coating the hybrids improved gloss levels. The effect of the hybrids in paper coating could be even further enhanced by utilizing fully exfoliated hybrid particles.

Overall, this study has shown that paper properties can be fine-tuned by hybrid and plastic pigments as they lie on top of the coating and paper surface. Only a handful of examples were demonstrated in respect to enhanced performance of paper by tailor-making plastic pigments for different applications with different requirements, *e.g.* hydrophilic or hydrophobic surface or increased weathering stability. Novel ideas could be searched for in research areas outside the traditional paper industry such as in the fields of medicine or electronics in order to develop new products and find new markets for paper.

6. References

(1) *Pigment Coating and Surface Sizing of Paper*; Lehtinen, E., Ed.; Fapet Oy: Helsinki, **2000**.

(2) *Pigments for paper*; Hagemeyer, R., Ed.; TAPPI press: Atlanta, **1997**.

(3) Gane, P.; Hooper, J.; Grunwald, A. *TAPPI Journal* **1997**, *80*, 109-115.

(4) Taber, D.; Stein, R. *TAPPI Journal* **1957**, *40*, 107-117.

(5) Li, J.; Tanguy, P. A.; Carreau, P. J.; Moan, M. *Colloid & Polymer Science* **2001**, *279*, 865-871.

(6) Conceição, S.; Santos, N.; Velho, J.; Ferreira, J. *Applied Clay Science* **2005**, *30*, 165-173.

(7) Ridgway, C. J.; Gane, P. A. C. *Journal of Dispersion Science and Technology* **2005**, *25*, 469.

(8) Al-Turaif, H.; Bousfield, D. W. *Progress in Organic Coatings* **2004**, *49*, 62-68.

(9) H. Murray, H.; Kogel, J. E. *Applied Clay Science* **2005**, *29*, 199-206.

(10) Al-Ani, T.; Sarapää, O. *Clay and clay mineralogy. Physical-chemical properties and industrial uses.*; GTK: Espoo, Finland, **2008**.

(11) Laufmann, M. In *PTS Seminarium: Wet end operations - Vorgänge in der Siebpartie*; Munich, Germany, **1998**; pp. 1-10.

(12) Laufmann, M. In *PTS Symposium: Chemische Technologie der Papierherstellung*; Munich, Germany, **1998**; pp. 1-10.

(13) Hagemeyer, R.; Welch, L. *TAPPI Journal* **1981**, *64*, 97-100.

(14) Hubbe, M. A. *The Book and Paper Group Annual* **2004**, *23*, 139-151.

(15) Woycheshin, E.; Sobolev, I. In *Handbook of Fillers and Reinforcements for Plastics*; Katz, H. S.; Milewski, J. V., Eds.; Van Nostrand Reinhold: New York, **1978**.

(16) Balan, E.; Lazzeri, M.; Morin, G.; Mauri, F. *American Minaralogist* **2006**, *91*, 115-119.

(17) El-Sherbiny, S.; Xiao, H. *Industrial & Engineering Chemistry Research* **2005**, *44*, 9875-9883.

(18) Alince, B.; Lepoutre, P. *Journal of Colloid and Interface Science* **1980**, *76*, 182-187.

(19) Heiser, E.; Shand, A. *TAPPI Journal* **1973**, *56*, 70-73.

(20) Pauler, N. *Paper optics*; Lorentzen & Wettre: Kista, Sweden, **1998**.

(21) Alince, B.; Lepoutre, P. *TAPPI Journal* **1980**, *63*, 49-53.

(22) Alince, B.; Lepoutre, P. *Colloids and Surfaces* **1983**, *6*, 155-165.

(23) Rennel, C.; Rigdahl, M. *Colloid Polymer Science* **1994**, *272*, 1111-1117.

(24) Lindblad, G.; Iversen, T.; Bergenblad, H.; Rigdahl, M. *Nordic Pulp and Paper Research Journal* **1989**, *4*, 253-257.

(25) Lee, D. I. *Progress in Organic Coatings* **2002**, *45*, 341-358.

(26) Liu, H.; Cao, K.; Huang, Y.; Yao, Z.; Li, B.; Hu, G. *Journal of Applied Polymer Science* **2006**, *100*, 2744-2749.

(27) Jeong, H.; Lee, B. -.; Cho, W. J.; Ha, C. -. *Polymer* **2000**, *41*, 5525-5529.

(28) Schmidt, U.; Zschoche, S.; Werner, C. *Journal of Applied Polymer Science* **2003**, *87*, 1255-1266.

(29) Sern, C. H.; May, C. Y.; Zakaria, Z.; Daik, R.; Foon, C. S. *European Journal of Lipid Science and Technology* **2007**, *109*, 440-444.

(30) Corato, R. D.; Quarta, A.; Piacenza, P.; Ragusa, A.; Figuerola, A.; Buonsanti, R.; Cingolani, R.; Manna, L.; Pellegrino, T. *Journal of Materials Chemistry* **2008**, *18*, 1991-1996.

(31) Moore, E.; Pickelman, D. *Industrial & Engineering Chemistry Product Research and Development* **1986**, *25*, 603-609.

(32) Lee, S.; Ahn, T. O. *Journal of Applied Polymer Science* **1999**, *71*, 1187-1196.

(33) Hu, G. H.; Lindt, J. T. *Polymer Bulletin* **1992**, *29*, 357-363.

(34) Liu, H.; Cao, K.; Yao, Z.; Li, B.; Hu, G. *Journal of Applied Polymer Science* **2007**, *104*, 2418-2422.

(35) Vermeesch, I.; Groeninckx, G. *Journal of Applied Polymer Science* **1994**, *53*, 1365-1373.

(36) Vermeesch, I. M.; Groeninckx, G.; Coleman, M. M. *Macromolecules* **1993**, *26*, 6643-6649.

(37) Dickinson, P. R.; Sung, C. S. P. *Macromolecules* **1992**, *25*, 3758-3768.

(38) Valton, E.; Schmidhauser, J.; Sain, M. *TAPPI Journal* **2004**, *3*, 25-30.

(39) Krakovský, I.; Lokaj, J.; Sedláková, Z.; Ikeda, Y.; Nishida, K. *Journal of Applied Polymer Science* **2006**, *101*, 2338-2346.

(40) Adler, H. P. In *Polymer Colloids*; Daniels, E. S., Ed.; ACS Symposium; American Chemical Society: Washington DC, US, **2001**; pp. 276-292.

(41) Kostansek, E. In *Polymer Colloids*; Daniels, E. S., Ed.; ACS Symposium; American Chemical Society: Washington DC, US, **2001**; pp. 13-22.

(42) Vanderhoff, J.; Park, J.; El-Asser, M. In *Polymer Latexes*; ACS symposium series; American Chemical Society: Washington DC, US, **1992**; pp. 272-281.

(43) Lee, D. M. *Fundamentals of emulsion polymerization: Binders for coated paper and paperboard. Coating Binders Short Course.*; TAPPI Coating & Graphic Arts Div., **1996**.

(44) Pham, H. H.; Kumacheva, E. *Macromolecular Symposia* **2003**, *192*, 191-206.

(45) Zou, M.; Wang, S.; Huang, F.; Zhang, Z.; Ge, X. *Polymer International* **2006**, *55*, 305-311.

(46) Okubo, M.; Kanaida, K.; Matsumoto, T. *Colloid & Polymer Science* **1987**, *265*, 876-881.

(47) Nakamura, H.; Tachi, K. *Journal of Applied Polymer Science* **2006**, *101*, 4153-4158.

(48) Borthakur, L. J.; Jana, T.; Dolui, S. K. *Journal of Coatings Technology and Research* **2010**, *7,* 765-772 .

(49) Vanderhoff, J. W. *Journal of Polymer Science, C Polymer Symposium* **2007**, *72*, 161-198.

(50) Jönsson, J.; Karlsson, O. J.; Hassander, H.; Törnell, B. *European Polymer Journal* **2007**, *43*, 1322-1332.

(51) Ito, F.; Ma, G.; Nagai, M.; Omi, S. *Macromolecular Symposium* **2002**, *179*, 257-274.

(52) Yong, C. S.; Neon, G. S. *Malaysian Journal of Chemistry* **2005**, *7*, 62-68.

(53) Tang, C.; Chu, F. *Journal of Applied Polymer Science* **2001**, *82*, 2352-2356.

(54) Stutman, D. R.; Klein, A.; El-Aasser, M. S.; Vanderhoff, J. W. *Industrial & Engineering Chemistry Product Research and Development* **1985**, *24*, 404-412.

(55) Landfester, K.; Boeffel, C.; Lambla, M.; Spiess, H. W. *Macromolecules* **1996**, *29*, 5972-5980.

(56) Pavlyuchenko, V.; Primachenko, O.; Sorochinskaya, O.; Ivanchev, S. *Russian Journal of Applied Chemistry* **2005**, *78*, 1987-1992.

(57) Chen, Y. C.; Dimonie, V.; El-Aasser, M. S. *Macromolecules* **1991**, *24*, 3779-3787.

(58) van Zyl, A. J. P.; Sanderson, R. D.; de Wet-Roos, D.; Klumperman, B. *Macromolecules* **2003**, *36*, 8621-8629.

(59) Zhao, K.; Sun, P.; Liu, D.; Wang, L. *Journal of Applied Polymer Science* **2004**, *92*, 3144-3152.

(60) Li, Z.; Yang, J.; Yu, Y.; Xu, X.; Meng, X.; Yu, W.; Xu, X.; Li, L.; Yue, X. *Journal of Applied Polymer Science* **2003**, *89*, 855-861.

(61) Gaillard, C.; Fuchs, G.; Plummer, C. J.; Stadelmann, P. A. *Micron* **2007**, *38*, 522-535.

(62) Torza, S.; Mason, S. G. *Journal of Colloid and Interface Science* **1970**, *33*, 67-83.

(63) McDonald, C. J.; Bouck, K. J.; Chaput, A. B.; Stevens, C. J. *Macromolecules* **2000**, *33*, 1593-1605.

(64) Pavlyuchenko, V. N.; Sorochinskaya, O. V.; Ivanchev, S. S.; Klubin, V. V.; Kreichman, G. S.; Budtov, V. P.; Skrifvars, M.; Halme, E.; Koskinen, J. *Journal of Polymer Science A Polymer Chemistry* **2001**, *39*, 1435-1449.

(65) McDonald, C. J.; Devon, M. J. *Advances in Colloid and Interface Science* **2002**, *99*, 181-213.

(66) Delgado, J. US Patent 5,053,436: Hollow acrylate polymer microspheres **1991**.

(67) Touda, H. US Patent 5,077,320: Microvoid-containing polymer particles **1991**.

(68) Okubo, M. US Patent 4,910,229: Process for producing hollow polymer latex particles **1990**.

(69) Kong, X.; Kan, C.; Li, H.; Yu, D.; Yuan, Q. *Polymers for Advanced Technologies* **1997**, *8*, 627-630.

(70) Kowalski, A.; Vogel, M. US Patent 4,469,825: Sequential heteropolymer dispersion and a particulate material obtainable therefrom, useful in coating compositions as an opacifying agent **1984**.

(71) Hitomi, H.; Toshiharu, E.; Fumihiko, O.; Yoko, S. *Japan TAPPI Journal* **2001**, *55*, 1599-1606.

(72) Zahradnik, M. *The Production and Application of Fluorescent Brightening Agents*; Wiley: Chichester, UK, **1982**.

(73) Roick, T. In *TAPPI 99 Proceedings*; TAPPI: Atlanta, **1999**; Vol. 2, pp. 821-828.

(74) Jokinen, O.; Baak, R.; Traser, G. In *PTS Coating symposium*; PTS: München, Germany, **1999**; p. 16E.

(75) Eklund, D.; Lindström, T. *Paper Chemistry - An Introduction*; DT Paper Science Publications: Grankulla, Finland, **1991**.

(76) Patrick, L. G. F.; Whiting, A. *Dyes and Pigments* **2002**, *55*, 123-132.

(77) Konstantinova, T. N.; Grabchev, I. K. *Polymer International* **1997**, *43*, 39-44.

(78) Bojinov, V.; Grabchev, I. *Dyes and Pigments* **2001**, *51*, 57-61.

(79) Jacquemin, D.; Perpète, E. A.; Scalmani, G.; Frisch, M. J.; Ciofini, I.; Adamo, C. *Chemical Physics Letters* **2007**, *448*, 3-6.

(80) Lewis, G. N.; Magel, T. T.; Lipkin, D. *Journal of the American Chemical Society* **1940**, *62*, 2973-2980.

(81) Singh, R. P.; Patwa, A. N.; Desai, S. M.; Pandey, J. K.; Solanky, S. S.; Prasad, A. V. *Journal of Applied Polymer Science* **2003**, *90*, 1126-1138.

(82) Gijsman, P.; Hennekens, J.; Tummers, D. *Polymer Degradation and Stability* **1993**, *39*, 225-233.

(83) Geuskens, G.; Kanada, M.; Nedelkos, G. *Bull. Soc. Chim. Belg.* **1990**, *99*, 1085-1100.

(84) Schaller, C.; Rogez, D.; Braig, A. *Journal of Coatings Technology and Research* **2009**, *6*, 81-88.

(85) Kaci, M.; Hebal, G.; Touati, N.; Rabouhi, A.; Zaidi, L.; Djidjelli, H. *Macromolecular Materials and Engineering* **2004**, *289*, 681-687.

(86) Jang, S.; Yi, S.; Hong, J. *Journal of Industrial Engineering Chemistry* **2005**, *11*, 964-970.

(87) Singh, R. P.; Prasad, A. V.; Pandey, J. K. *Macromolecular Chemistry and Physics* **2001**, *202*, 672-680.

(88) Rana, S.; Singh, R. P. *e-Polymers* **2007**, 1-7.

(89) Higuchi, A.; Hashiba, H.; Hayashi, R.; Yoon, B. O.; Sakurai, M.; Hara, M. *J Biomater Sci Polym Ed* **2004**, *15*, 1051-1063.

(90) Hwang, J. J.; Stupp, S. I. *Journal of Biomaterials Science, Polymer Edition* **2000**, *11*, 1023-1038.

(91) Shogren, R. L.; Willett, J. L.; Westmoreland, D.; Gonzalez, S. O.; Doll, K. M.; Swift, G. *Journal of Applied Polymer Science* **2008**, *110*, 3348-3354.

(92) Kakuchi, T.; Kusuno, A.; Shibata, M.; Nakato, T. *Macromolecular Rapid Communications* **1999**, *20*, 410-414.

(93) Willett, R. L.; Baldwin, K. W.; West, K. W.; Pfeiffer, L. N. *Proceedings of the National Academy of Sciences of the United States of America* **2005**, *102*, 7817-7822.

(94) Tavana, H.; Appelhans, D.; Zhuang, R.; Zschoche, S.; Grundke, K.; Hair, M.; Neumann, A. *Colloid & Polymer Science* **2006**, *284*, 497-505.

(95) Appelhans, D.; Wang, Z.; Zschoche, S.; Zhuang, R.; Haussler, L.; Friedel, P.; Simon, F.; Jehnichen, D.; Grundke, K.; Eichhorn, K.; Komber, H.; Voit, B. *Macromolecules* **2005**, *38*, 1655-1664.

(96) Tsuwi, J.; Appelhans, D.; Zschoche, S.; Zhuang, R.; Friedel, P.; Häußler, L.; Voit, B.; Kremer, F. *Colloid & Polymer Science* **2005**, *283*, 1321-1333.

(97) Gao, H.; Wang, D.; Guan, S.; Jiang, W.; Jiang, Z.; Gao, W.; Zhang, D. *Macromolecular Rapid Communications* **2007**, *28*, 252-259.

(98) Andersson, C. *Packag. Technol. Sci.* **2008**, *21*, 339-373.

(99) Deisenroth, E.; Jho, C.; Haniff, M.; Jennings, J. *Surface Coatings International Part B: Coatings Transactions* **1998**, *81*, 440-447.

(100) *Paper and Paperboard Converting*; Savolainen, A., Ed.; Fapet OY: Helsinki, **1998**.

(101) Schuman, T.; Adolfsson, B.; Wikström, M.; Rigdahl, M. *Progress in Organic Coatings* **2005**, *54*, 188-197.

(102) Jia, X.; Li, Y.; Zhang, B.; Cheng, Q.; Zhang, S. *Materials Research Bulletin* **2008**, *43*, 611-617.

(103) Sanchez, C.; Julian, B.; Belleville, P.; Popall, M. *Journal of Materials Chemistry* **2005**, *15*, 3559-3592.

(104) LeBaron, P. C.; Wang, Z.; Pinnavaia, T. J. *Applied Clay Science* **1999**, *15*, 11-29.

(105) Blanton, T.; Majumdar, D.; Melpolder, S. *Advanced X-Ray Analysis* **2000**, *42*, 562-568.

(106) Xia, H.; Song, M. *Polymer International* **2006**, *55*, 229-235.

(107) Lan, T.; Kaviratna, P. D.; Pinnavaia, T. J. *Chemistry of Materials* **1995**, *7*, 2144-2150.

(108) Sachan, A.; Penumadu, D. *Geotechnical and Geological Engineering* **2007**, *25*, 603-616.

(109) *Polymer-clay nanocomposites*; Pinnavaia, T. J.; Beall, G. W., Eds.; John Wiley & Sons Ltd: Chichester, UK, **2000**.

(110) Karesoja, M.; Jokinen, H.; Karjalainen, E.; Pulkkinen, P.; Torkkeli, M.; Soininen, A.; Ruokolainen, J.; Tenhu, H. *Journal of Polymer Science A Polymer Chemistry* **2009**, *47*, 3086-3097.

(111) Ammala, A.; Hill, A. J.; Lawrence, K. A.; Tran, T. *Journal of Applied Polymer Science* **2007**, *104*, 1377-1381.

(112) Elbokl, T. A.; Detellier, C. *Journal of Colloid and Interface Science* **2008**, *323*, 338-348.

(113) Elbokl, T. A.; Detellier, C. *Journal of Physics and Chemistry of Solids* **2006**, *67*, 950-955.

(114) Li, Y.; Zhang, B.; Pan, X. *Composites Science and Technology* **2008**, *68*, 1954-1961.

(115) Ledoux, R. L.; White, J. L. *Journal of Colloid and Interface Science* **1966**, *21*, 127-152.

(116) Rzhevskii, A. M.; Ribeiro, F. H. *Journal of Raman Spectroscopy* **2001**, *32*, 923-928.

(117) Wang, S.; Johnston, C. T. *American Mineralogist* **2000**, *85*, 739-744.

(118) Wolska, E.; Szajda, W. *Journal of Applied Spectroscopy* **1983**, *38*, 137-140.

(119) Saalfeld, H.; Wedde, M. *Zeitschrift für Kristallographie* **1974**, *139*, 129-135.

(120) Addai-Mensah, J. *Minerals Engineering* **1997**, *10*, 81-96.

(121) Mansour, S. H.; Iskander, B. A.; Nasrat, L. S. *Polymer-Plastics Technology & Engineering* **2006**, *45*, 857-863.

(122) Hapuarachchi, T.; Peijs, T. *Express Polymer Letters 3*, 743-751.

(123) Liu, P. *Applied Clay Science* **2007**, *38*, 64-76.

(124) Utracki, L. A.; Sepehr, M.; Boccaleri, E. *Polymers for Advanced Technologies* **2007**, *18*, 1-37.

(125) Agag, T.; Koga, T.; Takeichi, T. *Polymer* **2001**, *42*, 3399-3408.

(126) Delozier, D. M.; Orwoll, R. A.; Cahoon, J. F.; Johnston, N. J.; Smith, J. G.; Connell, J. W. *Polymer* **2002**, *43*, 813-822.

(127) Yano, K.; Usuki, A.; Okada, A. *Journal of Polymer Science Part A: Polymer Chemistry* **1997**, *35*, 2289-2294.

(128) Chang, J.; Park, D.; Ihn, K. J. *Journal of Applied Polymer Science* **2002**, *84*, 2294-2301.

(129) Park, C.; Smith Jr., J. G.; Connell, J. W.; Lowther, S. E.; Working, D. C.; Siochi, E. J. *Polymer* **2005**, *46*, 9694-9701.

(130) Gintert, M. J.; Jana, S. C.; Miller, S. G. *Polymer* **2007**, *48*, 4166-4173.

(131) Liang, Z.; Yin, J.; Xu, H. *Polymer* **2003**, *44*, 1391-1399.

(132) Yeh, J.; Hsieh, C.; Jaw, J.; Kuo, T.; Huang, H.; Lin, C.; Hsu, M. *Journal of Applied Polymer Science* **2005**, *95*, 1082-1090.

(133) Lin, H.; Chang, H.; Juang, T.; Lee, R.; Dai, S. A.; Liu, Y.; Jeng, R. *Dyes and Pigments* **2009**, *82*, 76-83.

(134) Mominul Alam, S. M.; Agag, T.; Kawauchi, T.; Takeichi, T. *Reactive and Functional Polymers* **2007**, *67*, 1218-1224.

(135) Kuan, H.; Ma, C. M.; Chuang, W.; Su, H. *Journal of Polymer Science Part B: Polymer Physics* **2005**, *43*, 1-12.

(136) Bae, W. J.; Kim, K. H.; Jo, W. H.; Park, Y. H. *Polymer* **2005**, *46*, 10085-10091.

(137) Xu, B.; Zheng, Q.; Song, Y.; Shangguan, Y. *Polymer* **2006**, *47*, 2904-2910.

(138) Schwarz, P.; Mahlke, M. In *TAPPI European PLACE Conference*; TAPPI: Rome, Italy, **2003**; pp. 1107-1136.

(139) Schuman, T.; Karlsson, A.; Larsson, J.; Wikström, M.; Rigdahl, M. *Progress in Organic Coatings* **2005**, *54*, 360-371.

(140) Sun, Q.; Schork, F. J.; Deng, Y. *Composites Science and Technology* **2007**, *67*, 1823-1829.

(141) *Pulp and paper testing*; Levlin, J.; Söderhjelm, L., Eds.; Fapet OY: Helsinki, **1999**.

(142) Preston, J. S.; Elton, N. J.; Husband, J. C.; Dalton, J.; Heard, P. J.; Allen, G. C. *Colloids and Surfaces A: Physicochemical and Engineering Aspects* **2002**, *205*, 183-198.

(143) Manski, S.; Mmbaga, J.; Hayes, R.; Bertrand, F.; Tanguy, P. In *Proceedings of the COMSOL Multiphysics User's Conference*; Boston, USA, **2005**.

(144) Havlínová, B.; Katuscák, S.; Petrovicová, M.; Maková, A.; Brezová, V. *Journal of Cultural Heritage* **2009**, *10*, 222-231.

ISBN 978-952-12-2599-4 (print)
ISBN 978-952-12-2600-7 (electronic)
Painosalama Oy – Turku, Finland 2011